SRC TR 88 - 32

MODELING of a COMMERCIAL FLUORESCENCE PROBE

by

Michael B. Simmons and
Nam Sun Wang

Modeling of a Commercial Fluorescence Probe

by

M. B. Simmons and N. S. Wang*

Department of Chemical and Nuclear Engineering
and System Research Center
University of Maryland
College Park, MD 20742

A Paper Presented at the AIChE 1987
Annual Meeting, November 15-20, New York.

* To whom correspondence should be addressed

Abstract

A model was developed which predicts the fluorescence signal measured by a commercial fluorescence probe which employs the back-scatter configuration, the signal being a function of the concentrations of fluorescing and absorbing components within the sample as well as the path length. The relationship is nonlinear in both the fluorophore concentration and the path length, due to inner-filter effects. An important parameter in the model is the exponential constant, S, which accounts for the variation in monitoring efficiency throughout the sample. The model prediction was verified for a single-component solution in which both the fluorophore concentration and path length were varied. An absorbance correction was developed which can be used to linearize the fluorescence relationship. Some aspects of multiple-component fluorescence are discussed as well as the expected effects of some environmental variables.

Introduction

A sterilizable probe which can monitor the fluorescence of a microbial fermentation has recently become commercially available from two manufacturers: Ingold, Inc. and BioChemTechnology, Inc. The operation of the probe is based on fluorescence of microbial cells within the fermentor. The probe was designed so that it could detect the fluorescnce due to the reduced cofactor, NADH, which is an electron carrier central to cells' energy metabolism. The fluorescence signal, however, is influenced by a number of factors. The manner in which these factors affect the fluorescence signal has not been well characterized. In this study, the response of this probe was modeled in oder to account for some of these factors. The model presented in this paper can be used as a basis for analyzing the fluorescence signal measured by the probe.

The Importance of NADH in Cellular Metabolism

NAD(P) and NAD(P)H are involved extensively as electron carriers in the oxidation/reduction (redox) reactions that comprise cellular metabolism. The vast majority of redox reactions employ either one or both forms of this cofactor. Chemotrophs always oxidize some type of substrate in order to obtain energy for cellular functions, including biosynthesis. When the substrate is oxidized, the reducing power of the substrate is stored for use by the cell by coupling the substrate oxidation with the reduction of a cofactor; directly or indirectly, this cofactor is NAD. For example, in organisms utilizing glucose for energy, the dehydrogenations of intermediate alcohols to aldehydes and aldehydes to carboxylic acids are coupled to the reduction of NAD to form NADH and to the reduction of NADP to form NADPH. Phototrophs reduce NAD(P) directly by using light energy. The reduction power needed for biosynthetic reactions is often provided by the reduced coenzyme itself. In organisms containing a respiratory chain, part of the reduction energy is saved by reducing a final electron accepter, such as oxygen, and coupling this redox chain of reactions with the phosphorylation of ADP to save the energy in the form of ATP. In terms of energy, NADH is very valuable. Depending on the respiratory chain involved, (i.e. the final electron accepter, number of phosphorylation sites, etc.) the oxidation of NAD(P)H can be worth up to three ATP's.[34] The dephosphorylation of NADPH is worth one additional ATP.

The standard oxidation-reduction potential of the half reaction involving NAD:

$$NAD^+ + 2H^+ + 2e^- \rightarrow NADH + H^+, \tag{1}$$

is -0.32 V.[30] Thus, NADH is a cofactor with relatively high reducing power. It is a loosely bound cofactor. During glycolysis, NAD is reduced to NADH via dehydrogenation of alcohols and aldehydes involved in the Embden-Meyerhoff pathway, for example, and the tricarboxylic acid cycle. Oxidation via the pentose phosphate cycle results in reduction of the phosphorylated form, NADP.

The reducing power of NADH can be shuttled to NADPH via a transhydrogenation reaction:

$$NADH + NADP^+ \rightarrow NAD^+ + NADPH. \quad (2)$$

Recycling of NAD is accomplished *partially* by the involvement of NADH and NADPH in biosynthetic reactions, especially those involving fatty acid and amino acid production. In fatty acid biosynthesis, the NADPH reduces a keto- moiety to a hydroxy- moiety and an enoate moiety to a fatty acid moiety. In amino acid biosynthesis, the reduction of keto- moieties to hydroxy- moieties is the predominant reaction involving NADH or NADPH. The remainder of the reduced NADH and NADPH is recycled via the reduction of an intermediate metabolite that is ultimately exported, in anaerobic cells, or via the reduction of an external electron accepter such as O_2, $NO_3^=$, $SO_4^=$, or even CO_2. The reduction of pyruvate to form lactate and the reduction of pyruvate to form ethanol are examples of anaerobic recycling of NAD. Organisms utilizing O_2 as the final electron accepter possess a respiratory chain with electron carriers including flavoproteins, cytochromes, and ubiquinone or meta-quinone(s).

In most respiratory chains, recycling NAD, electrons are first transferred from NADH to a flavoprotein. Flavoproteins are enzymes containing ether flavin adenine dinucleotide (FAD) or flavin mononucleotide (FMN) as a tightly bound cofactor. The standard oxidation/reduction potential is -0.22 V for FAD and -0.19 V for FMN [30]. The oxidation/reduction potentials for typical flavoproteins are close to these values and are greatly affected according to what proteins they are bound to. Thus, the flavoproteins have less reducing power than NADH. For this reason, the half reaction reducing FAD to $FADH_2$ is coupled to oxidative half reactions that involve species that do not have sufficient reducing power to reduce NAD. For example, the oxidation of fatty acids to enoate intermediates is coupled to FAD reduction, and succinate dehydrogenation in the tricarboxylic acid (TCA) cycle is also coupled to FAD reduction. In contrast, in the biosynthesis of fatty acids, the *reverse* of fatty acid oxidation, or reduction, is accomplished with the more reducing cofactor, NADPH, as mentioned above. Flavoproteins are also involved in oxidation reactions in which the flavoproteins are reduced and hydroxylation reactions with O_2 in which the flavoproteins are oxidized. Many flavoproteins, although not directly involved in the respiratory chain, are reduced by NADH.

There are a few electron carriers with more reducing power than NADH. For example, factor F_{420} and various ferredoxins have oxidation/reduction potentials of -0.37 V and -0.41 V, respectively. These cofactors are encountered when H_2 is produced or consumed, as in the assimilation of H_2 and CO_2 to form CH_4 in methanogens and the assimilation of H_2 and N_2 to form NH_3 in some nitrogen-fixing bacteria.

The extent that certain metabolic pathways are employed by a given organism depends greatly on the concentrations within the cells of the different forms of the cofactor: NADH, NADPH, NAD, and NADP. These cofactors are involved in many reactions where metabolic pathways diverge, or branch points. They may participate as either reactant, enzyme activator, enzyme inhibitor, or a combination of these. For example, as shown in Figure 1(a), many bacteria growing on glucose produce lactic acid under anaerobic conditions and oxidize glucose completely to CO_2 under aero-

bic conditions. The last common intermediate of these two pathways is pyruvate; thus, there is a branch point at pyruvate. The next step to form lactic acid is a reduction involving NADH, while the first step in the complete oxidation via the tricarboxylic acid cycle is oxidative decarboxylation of pyruvate, an oxidation step involving NAD. Beside this, NADH also inhibits the oxidative decarboxylation of pyruvate. There is a similar branch point found in the metabolism of brewer's yeast as shown in Figure 1(b). In this case, ethanol, instead of lactic acid, is produced under anaerobic conditions via a two-step process involving NADH in the second step.

A third example[14,15], shown in Figure 1(c), involves an intermediate in the biosynthesis of lysine in *Bacillus* species. 2,3-Dihydropicolinic acid is an intermediate in the biosynthesis of lysine. During sporulation, however, this intermediate is diverted to the production of dipicolinic acid (DPA), a major component of the spore coat. The intermediate in this case is either oxidized by NADP en route to DPA or reduced by NADPH en route to lysine. A high level of the coenzyme in the oxidized form would indicate substrate depletion, which is usually the cause for sporulation to occur, whereas a high level of the coenzyme in the reduced form would indicate biosynthetic capability.

As a final example, in *Escherichia coli*, many of the anaplerotic reactions replenishing TCA cycle intermediates utilized for biosynthesis, are allosterically controlled by NADH or NADPH [64,56]. An example of this is shown in Figure 1(d). Isocitrate, a TCA cycle intermediate, is a key intermediate which can either undergo oxidation as part of the cycle or undergo a lyase reaction which, along with the malate synthase reaction, acts as an anaplerotic sequence to replenish intermediates of the cycle. The oxidation reaction is inhibited by NADPH. The presence of NADPH indicates biosynthetic capability, so intermediates must be replenished in order to utilize this capability. In addition, NADPH indicates a reduced state in the cell, so that cycling of the TCA cycle will slow to allow re-oxidation of NAD(P)H via the respiratory chain to keep up with reduction of NAD(P) via the TCA cycle. In addition, two other TCA cycle enzymes that catalyze propagation of the cycle, malate dehydrogenase and citrate synthase, are also inhibited by NADH. Also, two enzymes which catalyze the consumption of TCA intermediates, the malic enzyme and phospho-enol pyruvate (PEP) carboxylase, are also inhibited by NADH.

The redox state of the NADH/NAD couple also indirectly affects cellular metabolism via the energy charge. When NADH/NAD is high, the energy charge, $\left(\frac{[ATP+\frac{1}{2}ADP]}{[ATP+ADP+AMP]}\right)$, is also high, since the NADH will drive the oxidative phosphorylation of ADP. The effects of the energy charge on cellular metabolism have been studied quite extensively, especially the effects on glycolysis and on the TCA cycle. Glycolysis and propagation of the TCA cycle are favored when the energy charge is low, while gluconeogenesis and other biosynthetic reactions are favored when the energy charge is high. In general, low energy and a low NADH/NAD ratio favor catabolic or energy producing pathways, while high energy charge and a high NADH/NAD ratio favor anabolic or energy consuming pathways.

Since NAD(P) and NAD(P)H have tremendous effects on various branch points of cellular

metabolism, knowing the concentrations of these cofactors can be very important for controlling and modeling the cellular metabolism of microorganisms. The fluorescence probe discussed in this paper has proved to have the capability of measuring the concentration of the reduced forms of these cofactors.

Utilization of NADH Fluorescence Measurement in Microbial Fermentations

The emission and excitation wavelengths of the reduced cofactors, NADH and NADPH, are 450 nm and 340 nm, respectively. These values are slightly changed upon binding of these cofactors to proteins as they are inside living cells. The oxidized cofactors do not fluorescence. This fact gives the fluorescence measurement the potential to be used to measure the internal reduction/oxidation state of the cofactors inside the cells. A typical fluorescence measurement involves excitation with an ultraviolet light source and detection of the fluorescent light emitted.

The fluorescence signal has been shown to depend on the biomass concentration as well as the NADH content of the cells [9,37]. Other factors affect the signal such as pH and temperature. See **Effect of Environmental Conditions on the Model Parameters** section of this paper. In addition, factors affecting optical path of the excitation and/or fluorescent light such as vessel geometry, bubbles due to aeration, and optical density of the medium itself will also affect the signal. (The basis for these effects will be revealed in the development of the model of fluorescence signal.) Finally, common medium constituents, such as yeast extract, casein, and peptone are highly fluorescent and interfere with the fluorescence measurement by increasing the background fluorescence and decreasing the sensitivity to NADH, cells, or any fluorophore in general. The sensitivity of the measurement is dependent upon the pH; and there is usually a pH corresponding to maximal sensitivity [9]. Generally, the sensitivity decreases with increasing temperature.

The most common application for the fluorescence measurement has been to estimate biomass concentration. It has the advantages over common methods of biomass estimation of being selective and instantaneous. Plate counts are most selective, but require a very long measurement lag, whereas, particulate matter found in most complex media often interferes with dry weight, optical density, and microscopic methods. The fluorescence measurement has been used to estimate biomass in fermentations of various organisms. Table 1 list the organisms whose concentration have been estimated with the fluorescence signal. In most cases, the biomass estimation was not the primary research objective. In these experiments, the pH, temperature, aeration, and vessel geometry were kept constant to prevent the effect that changes in these conditions would have on the fluorescence. Also, in most cases, the medium used did not contain any fluorophores, which would cause interference as stated above. The fluorescence did correlate well with biomass concentration during exponential growth in most cases. At low concentrations, a linear correlation can be used to fit the data. However, at higher concentrations, a nonlinear correlation must be used. Below are number

Table 1: Organisms Used for Biomass Estimation by NADH Fluorescence.

Saccharomyces cerevisiae [3,43,66,6,7,65,68,84,85,86]
Bacillus subtilis[54]
Bacillus amyloliquefaciens[83]
Candida tropicalis[6,7]
Candida utilis[82,62]
Escherichia coli[54,67,71,66,9]
Penicillium chrysogenum [70]
Streptomyces species [84,85,86]
Zymomonas mobilis [70]
Methylomonas mucosa [48]
Clostridium acetobutylicum [76,60]
Pediococcus species [10]
*Methanogenic bacteria [61,73]
Mouse fibroblast [10]
Mixed lymphocytes (B&T)[10]
Hybridoma[2]

*Based of the fluorescence of oxidized F_{420}.

---

of correlations that have been used to correlate biomass or cell count with fluorescence:

$X = K\Delta F$	(linear)*
$X = a + b\Delta F + c(\Delta F)^2$	(parabolic)[84,2,3,15]
$X = a'\Delta F^{b'}$	(log-log)[84,85,86,71]
$X = \alpha \exp(\beta\Delta F)$	(semi-log)[83,84,9]
$X = K'(\Delta F \cdot 10^{0.5(\mathrm{OD}_\lambda + \mathrm{OD}_{\lambda'})})$	(abs. corrected ($\perp$))[61]
$X = K''(\Delta F \cdot (\mathrm{OD}_\lambda + \mathrm{OD}_{\lambda'} + \mathrm{S}))$	(abs. corr. this work)
$X = \frac{\Delta F}{\alpha' - \Delta F \beta'}$	(this work)

* No references are cited since the net fluorescence signal is expected to be proportional to biomass at low concentrations.

In most cases, these correlations work well only during exponential growth [6]. All of these correlations, except the semi-log correlation, predict a linear correlation in the limit of low biomass concentrations. For this reason, the semi-log correlation will give erroneous results when used at low concentrations. However, one study suggests that there is a minimum biomass concentration (2 g/L for *B. subtilis*) below which no fluorescence signal can be detected [54]. The absorbance correction for the right-angle configuration accounts for absorbance of the excitation light and emission light which

both travel 0.5 cm to and from the center of the cuvette, respectively. The last two correlations will be suggested later in this paper.

In some cases the fluorescence does not correlate well with the biomass concentration. Reasons for this include low fluorescence of the cells, possibly accompanied by the uptake of an extracellular fluorophore, and secretion of an extracellular fluorophore [54]. These are the reasons for the lack of correlation in the cases of *Sporotrichum thermophile* and *E. coli* 5K, respectively, both transformed for the production of human leukocyte interferon [54]. Low cellular fluorescence may be the result of low levels of the pyridine coenzymes (both oxidized and reduced forms), NAD(P)(H). In a survey of twenty-two microorganisms, the level of these coenzymes within the cells was found to vary nearly two orders of magnitude, from 0.23 μmoles/g. dry wt. for *Psuedomonas fluorescens* to 11.1 μmoles/g. dry wt. for *Streptomyces faecalis* [46]. However, in a survey of the fluorescence of five types of bacteria at various excitation and emission wavelengths, *P. fluorescens* was found to be more fluorescent than *Staphylococcus epidermis*, *Enterobacter cloacae*, *E. coli*, and *B. subtilis* at the wavelengths corresponding to NADH fluorescence [20]. The high level of fluorescence in this case is known to be due to pteridin. This demonstrates that the fluorescence due to NADH may be a minor contribution to the total cellular fluorescence measured by systems tuned to detect NADH fluorescence. In particular, the fluorescence due to NADH in *S. cerevisiae* was estimated to be 50–60% of the total cellular fluorescence [84]. This is probably close to the upper limit for the relative contribution of NADH to the total cellular fluorescence since the NAD(P)(H) content of *S. cerevisiae*, 8.6 μmoles/g. dry wt., is relatively high (compared to that of other microorganisms) [46]. Oxygen-limitation is not required for a strong fluorescence signal. This has been demonstrated for *B. subtilis* [54].

The linear, log-log, and semi-log forms were used to correlate the culture fluorescence with the biomass concentration in batch fermentations of *S. cerevisiae* [84]. The log-log correlation was found to be the best, however, the data acquisition software used by the author employed a parabolic correlation to estimate the biomass concentration. It has been mentioned that constant temperature and pH as well as excessive substrate are required for the biomass correlation to hold [86]. See the **Effect of Environmental Factors on the Model Parameters** section of this paper for a discussion of other factors affecting the fluorescence signal.

In a study with *E. coli* ATCC 11105, the log-log correlation worked well in a batch stirred tank reactor [71]. However, different parameters were required when the fermentation was switched to a bubble-column reactor or made to be continuous. Further, the parameters for the continuous bubble-column fermentation didn't match those for the batch bubble-column fermentation. In this study, the biomass correlations for *E. coli* 5K in batch and continuous runs were compared. In the continuous runs, the fluorescence didn't correlate well with the biomass concentration. This was shown to be due largely to extracellular fluorescence. When the background fluorescence was subtracted, the correlation was similar to that in the batch runs, although there were other metabolic effects causing discrepancy. Further, when the gene for penicillin-G-acylase was incorporated, the

correlation was changed again. The steady-state fluorescence does not generally correlate with the steady-state biomass concentration in continuous fermentations as the dilution rate is varied due to changes in the internal metabolism [71,6,53].

Table 2 summarizes the various applications for which NAD(P)H fluorescence has been used.

Table 2: Applications for NADH fluorescence.

1. Determination of critical dissolved oxygen level.
2. Control of aeration or agitation to avoid anaerobiosis.
3. Measurement of substrate mixing, uptake, and utilization.
4. Recognition of metabolic transitions–substrate depletion, change of substrate, change from anaerobiosis to aerobiosis, product formation, etc.
5. Substrate feed-rate control to avoid glucose repression.
6. Biomass estimation.

See the Ingold Fluorosensor™: Theory and Applications manual [37] and the BioChem Technology FluroMeasure® System User's Guide [10] for a review of the applications of the NADH fluorescence probes.

Model Development

The Beer-Lambert law will be used along with idealized geometric approximations of the light-source/detector configuration, assuming a constant quantum yield of fluorescence. A sketch of the actual light-source/detector configuration in shown in Figure 2.

In order to simplify the analysis, an idealized approximation of the configuration is used. In this analysis, there are three levels of approximation. The simpler approximations have the advantage of being simple and containing few parameters. The more realistic approximations should be more accurate, however; and they reduce to the simpler approximations in special cases.

Preliminary experiments show that the simplest approximation is sufficiently accurate, but the parameters must be determined by curve-fitting. The more realistic approximations are also presented in order to elucidate problems with the simpler approximations. It could be advantageous to use the more complex analyses only if the additional parameters required can be obtained *a priori* and not determined by curve-fitting. Hopefully, less number of parameters must be obtained by curve-fitting when using the more complex analyses.

The first level of approximation assumes that the light source is located at a point in the center of the the probe tip window. The excitation light travels in a parallel beam perpendicular to the window surface. The emission light is reflected randomly in all directions. The fraction that is "seen" by the detector, considered to be the probe window, is determined by the size of the window

surface and the distance from the probe tip at which the fluorescence occurs. The distance that the emission light has to travel to reach the detector is assumed to be the distance to the *center* of the window on the probe tip. In order to determine the total amount of reflected light reaching the detector, the amounts of detected emission light resulting from fluorescence at various points are integrated over all possible distances, from $x = 0$ to $x = L$. Since fluorescence has arbitrary units, there is no need to scale the integral to keep units consistent.

At the second approximation level, the excitation light is considered to originate from a point at the center of the probe window as in the first approximation, but it is not considered to be a parallel beam, but it is considered to be a cone of light spread evenly over a cone angle, φ_{max}, such that the light intensity would be constant over any spherical surface bounded by φ_{max} with the point light source at the center. In this analysis it is noted that a circle, if viewed at an angle, appears as an ellipse. The detector is considered to be an "apparent" ellipse. The apparent ellipse is assumed to located at a distance from the point of reflection such that the major axis of the apparent ellipse is located in the actual circular disk representing the circular probe window. The amount of detectable reflected light originating from a locus of points defined by a distance from the probe tip, $x : 0 \leq x \leq L$, and a cone angle, $\varphi : 0 \leq \varphi \leq \varphi_{max}$ is determined as in the first approximation by assuming the average distance to be traveled by the reflected light to be equal to the distance to the center of the apparent ellipse. The apparent ellipse determines the fraction of the reflected light that is "seen" by the detector. In effect, for all points with a common x and φ, the apparent ellipse can be considered to be the actual probe window. Thus, the total fluorescence is obtained by integrating over all values of x and φ.

In the third level of approximation, the reflected light from a single point is not assumed to be the "average" distance from the probe tip, since the distance from the probe tip actually depends on the direction of the reflected light. In this analysis, the fluorescence is obtained by integrating over all values of x and φ, as well as integrating over all directions of the reflected light that are aimed toward the apparent ellipse, as discussed above.

A possible improvement at all three levels of approximation is to consider the detector surface to be the space between two concentric circles on the probe window, instead of a circular disk representing the entire probe window, since the actual detector is located in a ring around the tube where the excitation light travels outward. However, this improvement may not be necessary since the actual detector is recessed about 1 inch. Due to diffusion of light caused by the probe window, the actual point at which the light strikes the window is unimportant. (i.e. a constant fraction of light hitting the probe window also strikes the detector.) However, if necessary, this improvement is easily made at all three levels of approximation. In this development, any light detected resulting from multiple reflections is ignored. This light may result from the reabsorption and resultant fluorescence of scattered, reflected, or previously emitted light. *A procedure for accounting for this reabsorbed and reflected light will be presented elsewhere.*

According to the analysis presented in the following paragraphs, the most general approximation yields the following:

$$\Delta F = I_\lambda(0)\times$$
$$\frac{\int_0^L\int_0^{\varphi_{max}}\int_0^{2\pi}\int_{\varphi_1'(x,\varphi,\theta')}^{\varphi_2'(x,\varphi,\theta')}\sin\varphi\sin\varphi'\sum_{i=1}^{N}\phi_i a_{i,\lambda}c_i\left(\frac{I_\lambda(x)}{I_\lambda(0)}\right)\left(\frac{I_{\lambda'}(l_2)}{I_{\lambda'}(0)}\right)d\varphi'\,d\theta'\,d\varphi\,dx}{\int_0^{\varphi_{max}}\int_0^{2\pi}\int_0^{\pi}\sin\varphi\sin\varphi'\,d\varphi'\,d\theta'\,d\varphi} \tag{3a}$$

where

$$l_2 = l_2(x,\varphi,\theta',\varphi') \tag{3b}$$

and where

$$\left(\frac{I_\lambda(x)}{I_\lambda(0)}\right) = \exp\left(x\cdot\sum_{i=1}^{N}a_{i,\lambda}c_i\right) \tag{3c}$$

and

$$\left(\frac{I_{\lambda'}(l_2)}{I_{\lambda'}(0)}\right) = \exp\left(l_2\cdot\sum_{i=1}^{N}a_{i,\lambda'}c_i\right) \tag{3d}$$

if the Beer-Lambert law is applied.

The derivation of these equations and the meaning the variables used are presented below.

The angles, θ' and φ', are the circular and cone angles, respectively, in spherical coordinates corresponding to the emitted light using arbitrary references. Appropriate references will make the subsequent integration simpler. The limits $\varphi_1'(x,\varphi,\theta')$ and $\varphi_2'(x,\varphi,\theta')$ determine which light is aimed at the detector surface. If the detector surface is taken to be the entire probe window, then the lower limit will be zero (if the appropriate references are used). If the detector surface is taken to be the circular ring between two concentric circles, however, then the lower limit is a function of the other variables, just as the upper limit is. In the second level of approximation; $l_2 = l_2(x,\varphi)$ is used. The angle, φ, is the cone angle of the excitation light. The upper limit, φ_{max}, refers to the maximum spreading of the excitation light. Integrating over a spherical surface is appropriate since the intensity of light originating from a point source is constant over a spherical surface with the point source in the center of the sphere. There is no need to integrate over the circular angle for the excitation light because the light beam is assumed to be cylindrically symmetrical. *The details of the integration corresponding to the second and third levels of approximation will be presented elsewhere.*

In the first level of approximation, the integral over φ is not needed since the light is considered to be a collimated beam. Also, l_2 is considered to be equal to x, thus, the integral over θ' is unnecessary. The lower limit for φ' is zero, and the upper limit is $\tan^{-1}(R/x)$, where R is the radius of the effective detector surface. Thus, the equation reduces to:

$$\Delta F = \frac{1}{2}I_\lambda(0)\int_0^L\int_0^{\tan^{-1}(R/x)}\sin\varphi'\sum_{i=1}^{N}\phi_i a_{i,\lambda}c_i\left(\frac{I_\lambda(x)}{I_\lambda(0)}\right)\left(\frac{I_{\lambda'}(x)}{I_{\lambda'}(0)}\right)d\varphi'\,dx, \tag{4}$$

where the "$\frac{1}{2}$" results from the integral, $\int_0^{\pi} \sin\varphi' \, d\varphi' = 2$, in the denominator. Derivation of this form will be presented below. It is noted that the inner integral can be evaluated as follows:

$$\frac{1}{2}\int_0^{\tan^{-1}(R/x)} \sin\varphi' \ldots d\varphi' = \frac{1}{2}\left(1 - \frac{x}{\sqrt{x^2+R^2}}\right)\ldots \tag{5}$$

As a first approximation to the optical geometry of the probe, the following development assumes that the excitation light travels into the measurement vessel as a collimated beam. This light is absorbed according to Beer's Law by all components having absorbance at the excitation frequency (including all fluorophores). It is also assumed that all fluorophores emit an amount of light at the emission frequency that is proportional to the amount of excitation light that is absorbed.

According to the Beer-Lambert equation, the amount of light absorbed in a differential slice of fluid is proportional to the intensity of the incoming light at the excitation wavelength, $I_\lambda(x)$, the concentration of the absorbing species, c_i and the path length, dx. The amount of light absorbed by component i in the differential slice, dx, is given by:

$$-(dI_\lambda(x))_i = I_\lambda(x)\,(a_{i,\lambda}c_i)\,dx, \tag{6}$$

where $a_{i,\lambda}$ is the specific extinction coefficient for component i at wavelength λ.

The total amount of light absorbed in the differential slice is obtained by summing the amounts absorbed by each component. If there are N components:

$$-dI_\lambda(x) = -\sum_{i=1}^{N}(dI_\lambda(x))_i. \tag{7}$$

Substituting equation (6) into this equation gives:

$$-dI_\lambda(x) = I_\lambda(x)\cdot\sum_{i=1}^{N} a_{i,\lambda}c_i\,dx. \tag{8}$$

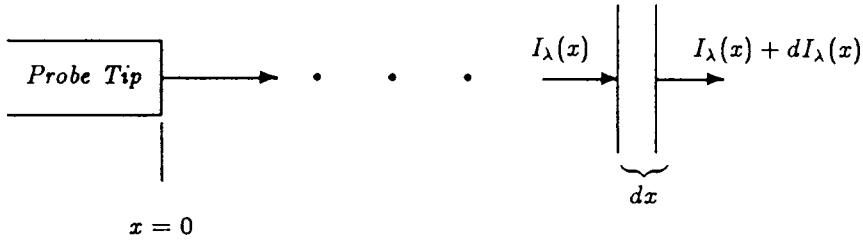

Integrating this equation gives the intensity of the excitation light as an explicit function of the distance from the probe tip, x, the intensity of the excitation light at the probe tip, $I_\lambda(0)$, the concentrations of the absorbing species and their specific extinction coefficients, $a_{j,\lambda}$:

$$I_\lambda(x) = I_\lambda(0)\cdot\exp\left[-x\cdot\sum_{j=1}^{N}(a_{j,\lambda}c_j)\right] \tag{9}$$

Substitution of this expression for $I_\lambda(x)$ in equation (6) yields an explicit function for the amount of light absorbed by each component, i, in the differential slice, dx:

$$-(dI_\lambda(x))_i = I_\lambda(0)e^{-x\cdot\sum_{j=1}^{N}(a_{j,\lambda}c_j)}\,(a_{i,\lambda}c_i)\,dx. \tag{10}$$

We will assume that the amount of light at the detected emission wavelength, λ', emitted by component i in the differential slice is proportional to the amount of excitation light (wavelength $= \lambda$) absorbed by that component in the slice. Let $\phi_{i,\lambda\to\lambda'}$ be the proportionality constant. If the component does not fluoresce, $\phi_{i,\lambda\to\lambda'} = 0$. If all wavelengths were being detected, $\phi_{i,\lambda\to ?}$ would be called the "quantum yield." We will refer to $\phi_{i,\lambda\to\lambda'}$ as the "fluorescence yield." The amount of light emitted by component i is given by:

$$(dE_{\lambda'})_i = \phi_{i,\lambda\to\lambda'}I_\lambda(0)\,(a_{i,\lambda}c_i)\cdot\exp\left(-x\cdot\sum_{j=1}^{N}(a_{j,\lambda}c_j)\right)dx. \tag{11}$$

Summing over all the fluorescent components, we obtain for the total fluorescence emitted in the differential slice by all components combined:

$$dE_{\lambda'} = \sum_{i=1}^{N}(dE_{\lambda'})_i = I_\lambda(0)\cdot\sum_{i=1}^{N}(\phi_i a_{i,\lambda}c_i)\exp\left[-x\cdot\sum_{j=1}^{N}(a_{j,\lambda}c_j)\right]dx. \tag{12}$$

The amount of this "reflected" light that makes it back to the detector is also given by the Beer-Lambert law. However, not all of the light is aimed back at the detector. As shown below in Figure 3, the cone angle, φ_2', which defines the fraction of the total light emitted by the fluorophore is a function of the distance from the probe tip, x. (Actually, each fluorophore molecule emits only one photon in only one direction, but we can assume each fluorophore molecule emits light in all directions by using the principle of a continuum.)

If the direction of the emitted light is completely random, then the fraction of the emitted light that is aimed toward the detector is equal to the fractional area of an arbitrary sphere that is bounded by the cone angle, φ_2', where φ_2' ranges from $\varphi_2' = 0$ as $x \to \infty$ to $\varphi_2' = \pi/2$ when $x = 0$. This area is equal to $2\pi x^2(1-\cos\varphi_2')$ where x is the radius of the sphere. The area of the entire sphere is equal to $4\pi x^2$. Thus, the fractional area is $\frac{1}{2}(1-\cos\varphi_2')$. Since $\cos\varphi_2' = \left(\frac{x}{\sqrt{x^2+R^2}}\right)$, where R is the radius of the probe tip, the fraction of emitted light that is directed toward the detector surface is given by:

$$f(x,R) = \frac{1}{2}\left[1-\frac{x}{\sqrt{x^2+R^2}}\right]. \tag{13}$$

This expression was obtained in equation (5) by evaluating the integrals with respect to φ'. Thus, the amount of "reflected" light in the differential slice that reaches the detector is given by:

$$dF_{\lambda'} = \frac{1}{2}\left\{1-\frac{x}{\sqrt{x^2+R^2}}\right\}\exp\left[-x\sum_{k=1}^{N}(a_{k,\lambda'}c_k)\right]dE_{\lambda'} \tag{14a}$$

or, after incorporating equation (12) and simplifying:

$$dF_{\lambda'} = \frac{1}{2} I_\lambda(0) \sum_{i=1}^{N} (\phi_{i,\lambda\to\lambda'} a_{i,\lambda} c_i) \left\{ 1 - \frac{x}{\sqrt{x^2+R^2}} \right\} e^{-x \sum_{j=1}^{N} (a_{j,\lambda} + a_{j,\lambda'}) c_j} dx. \tag{14b}$$

Integrating from $x = 0$ to $x = L$ gives the total light detected by the probe:

$$\Delta F = \frac{1}{2} I_\lambda(0) \cdot \sum_{i=1}^{N} (\phi_{i,\lambda\to\lambda'} a_{i,\lambda} c_i) \cdot \int_0^L \left\{ 1 - \frac{x}{\sqrt{x^2+R^2}} \right\} \exp\left[-x \cdot \sum_{j=1}^{N} (a_{j,\lambda} + a_{j,\lambda'}) c_j \right] dx. \tag{15}$$

The Δ is used because there may be a signal even if no fluorescent species are present, either due to external light sources or the calibration used.

In this analysis, it is assumed that the effect of light-scattering is similar to that of absorption in that once light is scattered, it can be assumed that it can no longer contribute to the detected fluorescence. In this case, the differential slice used in the analysis can be considered to have a radius such that any light leaving the area bounded by a circle with this radius will not contribute to the detected fluorescence. Back-scattered excitation light will have the effect of increasing the excitation light path length, while decreasing the emission light path length. Back-scattered emission light will have the opposite effect. However, due to light-scattering, the measured absorbancy will be higher than it really is. It is assumed that these effects will tend to cancel each, such that there a very small net effect will be observed. When there is a lot of light scattering, these assumptions will not be valid since light can be detected subsequent to multiple reflections. Since the emission light can take a tortuous path from the fluorophore to the detector, the factor, $f(x, R)$, will have a larger effective value than predicted above. For the same reason, the effective path length will be longer. The same is true for the excitation light.

To account for small amounts light scattering by various mechanisms, unmeasurable but constant absorption, and divergence of the excitation light source, a constant, S, is added to the absorption terms in the exponential. The contribution of background absorbance will certainly result in a constant term. The contribution due to light scattering and divergence the excitation light would be considered constant if the amount of light leaving through the back and sides of a constant-width differential slice of fluid is proportional to the amount of light entering the differential slice through the back.

In order to integrate equation (15) analytically, it will be assumed that the effect of the f factor can be approximated by incorporating the effect into the parameter, S. In effect, $\left(1 - \frac{x}{\sqrt{x^2+R^2}}\right)$ is approximated by e^{-xS}. The parameter, S, then, is not actually a constant, but is given by:

$$S = -\left\{ \frac{\log\left(1 - \frac{x}{\sqrt{x^2+R^2}}\right)}{x} \right\}. \tag{16}$$

In Figure 4, S is plotted as a function of x for $R = 1\,\text{cm}$, which is approximately the radius of the probe tip. Over the region from $x = 0\,\text{cm}$ to $x = 5\,\text{cm}$, the approximation has a maximum relative error of only 25 percent. The approximation does not have to be accurate for values of x greater than about 5 cm because most of the fluorescence occurs much closer to the probe tip than this. Note that there may be other contributions beside the "f" factor to the parameter, S. All the contributions to S will be discussed in more detail in the next section. Lumping this effect and all the effects listed above into the parameter, S, we get:

$$\Delta F = \frac{1}{2} I_\lambda(0) \sum_{i=1}^{N} \left(\phi_{i,\lambda\to\lambda'} a_{i,\lambda} c_i\right) \int_0^L e^{-x\left[\sum_{j=1}^{N}\left(a_{j,\lambda}+a_{j,\lambda'}\right)c_i+S\right]} dx \tag{17a}$$

or, after evaluating the integral:

$$\Delta F = \frac{\frac{1}{2} I_\lambda(0) \sum_{i=1}^{N} \left(\phi_{i,\lambda\to\lambda'} a_{i,\lambda} c_i\right) \left[1 - e^{-L\left[\sum_{j=1}^{N}\left(a_{i,\lambda}+a_{i,\lambda'}\right)c_i+S\right]}\right]}{\sum_{i=1}^{N}\left(a_{i,\lambda} c_i + a_{i,\lambda'} c_i\right) + S}. \tag{17b}$$

The validity of approximating $f(x, R)$ with an exponential factor can be examined by comparing the predicted fluorescence signal for equations (15) and (17b) using typical values for the constants. The following values for were used to evaluate equation (15): $N = 1$; $\frac{1}{2} I_\lambda(0) = 200$; $\phi_{1,\lambda\to\lambda'} = 0.0556$; $a_{1,\lambda} = 0.09$; $a_{1,\lambda'} = 0.01$; and $R = 1.0\,\text{cm}^{-1}$. Concentration, absorbance, light-intensity and fluorescence units are arbitrary. Unit length is assumed to be 1 cm. In Figure 5, equation (15) is compared with equation (17b), using $S = 1/R = 1\,\text{cm}^{-1}$, as suggested in the subsection of this paper entitled Estimation of the Light Scattering Parameter, S. It is noted that both expressions predict a linear relationship between concentration and fluorescence at low concentrations and short path lengths, L. Also, as the concentration increases, both expressions predict the fluorescence to level off at a value of $\left(\frac{\frac{1}{2} I_\lambda(0)\phi_{1,\lambda\to\lambda'} a_{1,\lambda}}{a_{1,\lambda}+a_{1,\lambda'}}\right)$. In this example the maximum fluorescence value is 10. These two expressions agree to within 10%. Since equation (17b) always overestimates the predicted fluorescence obtained using by equation (15), a better agreement is obtained using a slightly higher value of S. Thus, for $S = 1.2\,\text{cm}^{-1}$, the agreement is almost perfect, as shown in Figure 6.

If the fermentor is deep enough, the exponential term can be ignored, simplifying the equation to:

$$\Delta F = \frac{\frac{1}{2} I_\lambda(0) \cdot \sum_{i=1}^{N} \left(\phi_{i,\lambda\to\lambda'} a_{i,\lambda} c_i\right)}{\sum_{i=1}^{N}\left(a_{i,\lambda} + a_{i,\lambda'}\right) c_i + S}. \tag{18}$$

Figure 7 shows how deep the fermentor needs to be in order to be considered infinitely deep, using the same constants as in Figure 5.

In this case, the fermentor can be considered infinitely deep if $L > \approx 2\,\text{cm}$.

There is considerable relative error at very low concentrations since the error is proportional to $\left(e^{-a_{\lambda,1} c_1 L}\right)$. Thus, this model shows that the relationship between fluorescence and fluorophore concentration is nonlinear, but this is at least not completely due to signal saturation. Instead, absorbance at both the excitation and emission wavelengths as well as the decreasing of f as x increases cause the nonlinearity of the fluorophore-fluorescence relationship.

For a single fluorescent species in solution, the model predicts the following relationship:

$$\Delta F = \frac{\frac{1}{2} I_\lambda(0) \phi_{\lambda \to \lambda'} a_\lambda c}{(a_\lambda + a_{\lambda'}) c + S} \left[1 - \exp\left(-L\left[(a_\lambda + a_{\lambda'}) c + S\right]\right)\right]. \tag{19}$$

This relationship has been evaluated experimentally using thioflavin S as the fluorescent species, varying both the concentration as well as the path length. The agreement is quite good, but the model parameters don't have the values that they are predicted to have. See the **Model Verification and Application** section of this paper.

In order to use the model to correlate fluorescence with biomass concentration, we can assume that the fermentor is sufficiently deep so that equation (19) can be used. If the cells are the only fluorophores present, then using X to denote cell concentration, we have:

$$\Delta F \approx \frac{\frac{1}{2} I_\lambda(0) \phi_{X,\lambda \to \lambda'} a_{X,\lambda} \cdot X}{S + \sum_{i=2}^{N} (a_{i,\lambda} + a_{i,\lambda'}) c_i + (a_{X,\lambda} + a_{X,\lambda'} + S_X) X}. \tag{20}$$

where the term, $\sum_{i=2}^{N} (a_{i,\lambda} + a_{i,\lambda'}) c_i$, results from absorbance of all other components at the excitation and emission wavelengths. Some features of this relationship are noted. First, at low cell concentrations, the relationship is linear. This is either due to the predominance of the S term, indicating light scattering and dispersion, or the predominance of the summation, indicating absorbance at the excitation and/or emission frequency by components other than the cells. Secondly, compounds that absorb either the emission light or the excitation light decrease the sensitivity of the fluorescence measurement. Light scattering decreases the sensitivity also, as well as the cells themselves. Finally, there is a maximum fluorescence equal to $\left[\frac{1}{2} I_\lambda(0) \phi_{X,\lambda \to \lambda'} \left(\frac{a_{\lambda,X}}{a_{\lambda,X} + a_{\lambda',X} + S_X}\right)\right]$. Using the form of equation (20), the biomass concentration can be correlated as follows:

$$\Delta F = \frac{\alpha X}{1 + \beta X}. \tag{21}$$

where $\alpha = \dfrac{\frac{1}{2} I_\lambda(0) \phi_{X,\lambda \to \lambda'} a_{X,\lambda}}{S + \sum_{i=2}^{N} (a_{i,\lambda} + a_{i,\lambda'}) c_i}$ and $\beta = \dfrac{a_{X,\lambda} + a_{X,\lambda'} + S_X}{S + \sum_{i=2}^{N} (a_{i,\lambda} + a_{i,\lambda'}) c_i}$.

If there *are* other fluorophores present, the relationship is:

$$\Delta F \approx \frac{\frac{1}{2} I_\lambda(0) \left(\phi_X a_{X,\lambda} X + \sum_{i=2}^{N} (\phi_i a_{i,\lambda} c_i)\right)}{S + \sum_{i=2}^{N} (a_{i,\lambda} + a_{i,\lambda'}) c_i + (a_{X,\lambda} + a_{X,\lambda'} + S_X) X}. \tag{22}$$

Other fluorophores have the effect of adding background to the signal as well as decreasing the sensitivity of the signal due to the absorbance of excitation light by the fluorophore. The biomass can be correlated using the following form:

$$\Delta F = \frac{\alpha X + F_0}{1 + \beta X}, \tag{23}$$

where α and β are the same as above, and F_0 is the measured background fluorescence equal to $\dfrac{\frac{1}{2} I_\lambda(0) \sum_{i=2}^{N} (\phi_{i,\lambda \to \lambda'} a_{i,\lambda} c_i)}{S + \sum_{j=2}^{N} (a_{j,\lambda} + a_{j,\lambda'}) c_j}$. The parameters F_0, α, and β vary with the background fluorophore

concentration. However, the ratio α/β, which is the maximum fluorescence as X increases, remains constant. If the background fluorescence, F_0, is constant, the difference between the measured fluorescence and the background fluorescence, $\Delta F' = \Delta F - F_0$, can be expressed as:

$$\Delta F' = \frac{(\alpha - F_0\beta)X}{\beta X + 1} = \frac{\alpha' X}{\beta X + 1}. \tag{24}$$

which is the same form as for the case in which the biomass is the only fluorophore present.

If the amount of background fluorescence changes, but it is assumed to be constant, there will be an error in the estimation of the concentration of the primary fluorophore. Equation (24) was used to evaluate the error caused by a 10% decrease in the concentration of a secondary fluorophore, assuming only these species are fluorescence and that only these two species absorb light at either the emission or excitation wavelength. The primary fluorophore was assumed to have the same extinction coefficients and fluorescent yield as used in Figures 5-7 ($a_{1,\lambda} = 0.09$, $a_{1,\lambda'} = 0.01$, and $\phi_{1,\lambda\to\lambda'} = 0.0556$). The parameter, S, was set to $1.0\,\mathrm{cm}^{-1}$, and $\frac{1}{2}I_\lambda(0)$ was set to 200. Figure 8 summarizes the results of this analysis. The error in the estimate of the concentration of the primary fluorophore caused by a 10% overestimate of the secondary fluorophore concentration is plotted against the primary fluorophore concentration for the cases in which $\phi_2 = \phi_1$, $\phi_2 = 10\phi_1$, and $\phi_2 = 0.1\phi_1$. The concentrations of the two components are such that the fluorescence signals that each component would have in the absence of the other component are equal. If the fluorescent yield of the secondary component is equal to that of the primary component, a 10% decrease in the secondary component concentration will result in an over estimation of the primary fluorophore concentration by 10% since the the sensitivities of the two components are equal. However, if the fluorescent yield of the secondary fluorophore is greater than that of the primary fluorophore, then the overestimate is much more severe. This is because the fluorescence signal is more sensitive to the second component than it is to the first component. As the concentrations are increased, the sensitivity to the concentration of the first component approaches zero. There comes a point at which an infinite concentration of the primary component is required to make up the fluorescence lost by the 10% drop in the secondary component concentration. This corresponds to the vertical assymptote in Figure 8. Above this concentration, negative concentration of component is predicted. If the fluorescent yield of the secondary component is less than that of the primary component, the estimate is off by less than 10%, changing from a positive error to a negitive error. The lower relative error results because the fluorescence signal is less sensitive to the concentration of the secondary component than it is to the concentration of the primary component. The negative error results because of the filtering caused by the secondary component. See below. The error becomes negative when equation (25) is satisfied.

The type of correlation indicated by equation (24) was evaluated for estimating the sensitivity to NADH in the presence of various fluorescent medium components. See **Model Verification and Application** section of this paper. If $\alpha > F_0\beta$, then equation (24) is the same as equation (21) with $\alpha' = \alpha - F_0\beta$. If $\alpha < F_0\beta$, the fluorescence is predicted to decrease with cell concentration. This

is a result of the less fluorescent species, the cells, blocking the light (by absorption) to the more fluorescent background component(s). This type of phenomena has not been reported for culture fluorescence studies thus far. In the case where only one background fluorophore is present, denoted component 1, the prerequisite for this phenomena to be observed is that:

$$S + (a_{X,\lambda} + a_{X,\lambda'})c_X < \left(\phi_1 - \phi_X \left(\frac{a_{1,\lambda} + a_{1,\lambda'}}{a_{1,\lambda}}\right)\right) a_{1,\lambda} c_1. \tag{25}$$

Thus, this phenomena can be observed by increasing the concentration of the background fluorophore, c_1, as long as:

$$\phi_1 > \left(\frac{a_{1,\lambda} + a_{1,\lambda'}}{a_{1,\lambda}}\right) \cdot \phi_X. \tag{26}$$

Thus, the fluorescence yield must be higher for the background component in order to observe a decrease in the fluorescence signal upon addition of an additional fluorophore.

Estimation of the Light-Scattering Parameter, S

The contributions to the parameter, S, are as follows: (1) divergence of excitation light, (2) divergence of emission light, (3) scattering of excitation light, (4) scattering of emission light, (5) solvent absorbance of excitation light, and (6) solvent absorbance of emission light, or

$$S = S_{diverg.,\lambda} + S_{diverg.,\lambda'} + S_{scat.,\lambda} + S_{scat.,\lambda'} + S_{solv.,\lambda} + S_{solv.,\lambda'}. \tag{27}$$

Light-scattering due to reflection of light of the vessel walls and agitator blades is very dependent on the specific vessel configuration and is not considered here.

$S_{solv.}$ is any absorbance of light by the reference solvent (usually water) used to zero the spectrophotometer when measuring the absorbance. Water is extremely transparent to visible light, so $S_{solv.,\lambda'} \approx 0$. However, $S_{solv.,\lambda}$ may be nonzero. $S_{scat.}$ accounts for light-scattering due to particulate matter, bubbles or suspension of a second liquid phase. It is expected that this value will increase as the number of bubbles increases and as the number of cells and/or other particles increases. The value of $S_{scat.}$ will be less dependent on the light wavelength than absorbance terms. *The effect of light-scattering will be investigated in more detail elsewhere.*

It was mentioned earlier that the fraction of the emission light that is aimed back at the detector surface, having a radius equal to R, is given by $f(x,R) = \frac{1}{2}\left(1 - \frac{x}{\sqrt{x^2+R^2}}\right)$. Let us now estimate what value of $S_{diverg.}$ will best approximate the expression for f. In our model, the fraction of light reflected back to the detector is given by $f = \frac{1}{2} \cdot \exp(-xS_{diverg.})$. Therefore, we have:

$$\exp(-xS_{diverg.}) \approx 1 - \frac{x}{\sqrt{x^2+R^2}}. \tag{28}$$

Note that these two expressions have the same limits as $x \to 0$ and $x \to \infty$. In order to estimate the best value for $S_{diverg.}$, it is desired to minimize the absolute value of the difference between the two expressions integrated from $x = 0$ to $x = \infty$. Thus, the best value of $S_{diverg.}$ will minimize the following function:

$$g(S_{diverg.}) = \int_0^\infty \left|1 - \frac{x}{\sqrt{x^2+R^2}} - \exp(-x \cdot S_{diverg.})\right| dx. \tag{29}$$

Integrating this expression leads to a nonlinear optimization problem with a nonlinear constraint. This is too complicated to solve analytically, but a simpler criterion can be used to solve analytically for an optimal value of $S_{diverg.}$. Equating the integral of the two expressions from $x = 0$ to $x = \infty$ gives:

$$\int_0^\infty \left(1 - \frac{x}{\sqrt{x^2 + R^2}}\right) dx = \int_0^\infty \exp\left(-xS_{diverg.}\right) dx \tag{30a}$$

or

$$S_{diverg.} \approx \frac{1}{R}. \tag{30b}$$

For example, in Figures 5 and 6, the detector radius, R, was assumed to be 1 cm. In Figure 5, $S_{diverg.,\lambda'} = \frac{1}{R} = 1.0\,\mathrm{cm}^{-1}$ was used. However, in Figure 6, a slightly higher value, $S_{diverg.,\lambda'} = 1.2\,\mathrm{cm}^{-1}$ was used with much better results.

The expression above accounts for divergence of the emission light. The divergence of the excitation light depends on how the light is focused. If the excitation light is a straight beam perpendicular the detector surface originating from a point in the center of the probe tip, then $S_{diverg.,\lambda} = 0$. Otherwise, it is nonzero. We will estimate $S_{diverg.,\lambda}$ by assuming that the excitation light originates from a point in the center of the probe tip and spreads evenly over a cone angle, φ_{max}, as shown in Figure 9. In order to estimate the effect that the spreading of the excitation light would have on the value of $S_{diverg.,\lambda}$, the second level of approximation will be used. *This analysis will be presented elsewhere in the near future.*

Results and Discussion

Model Verification and Application

Controlled experiments with thioflavin S:

In order to test the validity of the model, thioflavin S was used as a standard fluorophore. The advantage of using this compound, as opposed to NADH, for example, is that this compound is stable, cheap, and has a high fluorescent yield. The concentration of thioflavin S as well as the path length, L were varied. The later effect was accomplished by positioning a black disc a distance, L, from the probe as shown in Figure 10.

Although L is almost always fixed in a fermentor, varying L permitted evaluation of the model parameters and also indicated how deep the fermentor would need to be to be considered "infinitely deep."

The equation derived in the previous section to describe the fluorescence signal expected from only one fluorophore when no other components in the solution absorb light at the excitation or the emission frequency is:

$$\Delta F = \frac{\frac{1}{2} I_{340}(0) \phi_{340 \rightarrow 450} a_{340} c}{(a_{340} + a_{450})\, c + S} \left[1 - \exp\left(-L\left[(a_{340} + a_{450})\, c + S\right]\right)\right]. \tag{19}$$

Actually there are only two unknown parameters in this equation, $\frac{1}{2} I_{340}(0) \phi_{340 \rightarrow 450}$ and S, however, it can be made more flexible if only the form the equation is retained, not requiring the coefficients to equal the values specified in the analysis. See **Discussion of Preliminary Results** section to see why a more flexible form of this correlation may be required. The following equation was fit from the experimental results:

$$\Delta F = \frac{k_1 \cdot c}{(k_2 \cdot c + S)} \left[1 - \exp\left(-L\,(k_2 \cdot c + S)\right)\right]. \tag{31}$$

Note that all the constants cannot be determined unless L is varied. For example, if $L \rightarrow \infty$, then only the ratios (k_1/S) and (k_1/k_2) can be determined by varying c.

According to equation (31), at constant fluorophore concentration, the fluorescence data can be correlated with the path length as follows:

$$\Delta F = F_{max}\left[1 - \exp\left(-kL\right)\right] \tag{32}$$

The best values for F_{max} and k were determined for each of four different concentrations of thioflavin S as shown in Figure 11.

Both of theses parameters can be correlated with the fluorophore concentration as follows:

$$F_{max} = \frac{k_1 c}{k_2 c + S} \tag{33}$$

and

$$k = k_2 c + S. \tag{34}$$

If linear regression is to be used, there are two methods to find the best values for k_1, k_2, and S. In the first method, it is possible to determine the best values for k_1, k_2, and S, by first plotting k versus c in order to determine k_2 and S as the values of the slope and intercept, respectively, of the best line to fit the data. Finally, the best value for k_1 can be found by substituting k_2 and S into equation (33) and plotting $F_{max}(k_2 + K_3 c)$ versus c, finding the best line that passes through the origin. The slope of this line will be equal to k_1. Alternatively, $(1/F_{max})$ can be plotted versus $(1/c)$. The slope and intercept of the best line are equal to (S/k_1) and (k_2/k_1), respectively. Next, k is plotted versus $\left[\left(\frac{S}{k_1}\right) + \left(\frac{k_2}{k_1}\right) c\right]$, finding the best line through the origin. Again, the slope will be equal to k_1. The results of these two methods were compared using least square criterion on the difference between the fluorescence signal predicted by equation (31) and that measured experimentally.

In this case, the *second* method gives slightly better results, but they are not significantly better than the results from the first method. The correlation the exponential constants, F_{max} and k, according to the *first* method are shown in Figures 12 and 13. Finally, in Figure 14, the fluorescence is correlated with both the concentration and path length according to equation (31).

The values obtained for the constants:

$$S = 0.412\,\mathrm{cm}^{-1}, \qquad k_1 = 60.3\,\frac{\mathrm{NFU}}{\mathrm{cm\ ppm}}, \quad \text{and} \quad k_2 = 0.0172\,\mathrm{cm}^{-1}\mathrm{ppm}^{-1}, \tag{35}$$

were obtained using the second method of linear regression. The average deviation of this correlation is within the experimental deviation of the fluorescent signal itself. However, the value of k_2 was larger than the value expected from the model, $(a_{340} + a_{450})$. In the section, **Discussion of Preliminary Results**, possible reasons for the discrepancy are discussed. Among the reasons discussed is the possibility that there are other sources of nonlinearity. In order to eliminate the effect of these other sources, the experiment was repeated with lower concentrations of thioflavin S, varying from 1 ppm to 6 ppm. The results of the second experiment are shown in Figures 15 to 18. Caution should be used when comparing the results of two experiments because a different source of thioflavin S was used in the two experiments. Also, the probe was modified between the two experiments, resulting in a narrower bandwidth of both the excitation and emission light and possible changes in the focusing of the excitation light and in the viewing field of the detector.

It is noted that F_{max} is nearly linear with concentration over this small range of concentrations, such that the value of S has little effect on F_{max}. In addition, the correlation of the exponential constant, k, is not as good as in the first experiment. This is probaly due to absolute errors in the fluorescence signal, which are a larger fraction of the total signal when the concentration is low.

In the very near future, other fluorophores will be employed along with nonfluorescent substances that absorb light at the excitation frequency and/or excitation frequency to further test the model. In particular, it will be interesting to see how S and k_2 vary these conditions. It was estimated that,

for the probe being studied, $R \approx 0.75\,\text{cm}$. The estimated value of S in this case is

$$S = S_{diverg.,450} + \ldots \approx \frac{1}{R} + \ldots \approx 1.33\,\text{cm}^{-1}. \tag{36}$$

This estimated value of S is little more than three times the experimentally determined value. The possible reasons for this will be discussed in the **Discussion of Preliminary Results** section.

Application to published culture and NADH fluorescence data:

Equation (22) was used to correlate previously published culture fluorescence and NADH calibration data [9]. The effect of background fluorescence of various media was studied. In this study, the sensitivity of the fluorescence signal to NADH, $\frac{\partial \Delta F}{\partial [\mathrm{NADH}]}$, in various media and the media background fluorescence have been reported. In order to correlate the sensitivity data, equation (17) is written for the case of only two components, where 1 denotes NADH and 2 denotes the background fluorophore:

$$\Delta F = \frac{\frac{1}{2} I_\lambda(0) \phi_{1,\lambda \to \lambda'} a_{1,\lambda} c_1 + \frac{1}{2} I_\lambda(0) \phi_{2,\lambda \to \lambda'} a_{2,\lambda} c_2}{S + (a_{1,\lambda} + a_{1,\lambda'}) c_1 + (a_{2,\lambda} + a_{2,\lambda'}) c_2}. \tag{37a}$$

or

$$\Delta F = \frac{\alpha_1 c_1 + \alpha_2 c_2}{S + \beta_1 c_1 + \beta_2 c_2} \tag{37b}$$

where $\alpha_1 = \frac{1}{2} I_\lambda(0) \phi_{1,\lambda \to \lambda'} a_{1,\lambda}$, $\alpha_2 = \frac{1}{2} I_\lambda(0) \phi_{2,\lambda \to \lambda'} a_{2,\lambda}$, $\beta_1 = a_{1,\lambda} + a_{1,\lambda'}$, and $\beta_2 = a_{2,\lambda} + a_{2,\lambda'}$. In the absence of NADH, the background fluorescence is:

$$\Delta F = \frac{\alpha_2 c_2}{S + \beta_2 c_2} \tag{38}$$

Thus, a plot of $(1/\Delta F)$ versus $(1/c_2)$ should be a straight line with a slope of (S/α_2) and an intercept of (β_2/α_2). This correlation is plotted in Figures 19 and 20 for various medium components.

The sensitivity to NADH at zero concentration can be expressed as follows:

$$\left.\frac{\partial \Delta F}{\partial c_1}\right)_{c_1 = 0} = \frac{\alpha_1 S + (\alpha_1 \beta_2 - \alpha_2 \beta_1) c_2}{(S + \beta_2 c_2)^2} \tag{39}$$

Dividing the top and bottom of this equation by α_2^2, we get:

$$\left.\frac{\partial \Delta F}{\partial c_1}\right)_{c_1 = 0} = \frac{\left(\frac{\alpha_1 S}{\alpha_2^2}\right) + \left(\frac{\alpha_1 \beta_2 - \alpha_2 \beta_1}{\alpha_2^2}\right) c_2}{\left(\frac{S}{\alpha_2} + \frac{\beta_2}{\alpha_2} c_2\right)^2} \tag{40}$$

The terms, (S/α_2) and (β_2/α_2) were evaluated from the background fluorescence correlation. The sensitivity to NADH when $c_2 = 0$ is equal to 121.3 $\left(\frac{\mathrm{NFU}}{2\,\mathrm{mg\ NADH}}\right)$. This is predicted to be equal to (α_1/S). Thus, the term $(\alpha_1 S/\alpha_2^2)$ equals 121.3 $\left(\frac{\mathrm{NFU}}{2\,\mathrm{mg\ NADH}}\right) \cdot \left(\frac{S}{\alpha_2}\right)^2$. The term, $\left(\frac{\alpha_1 \beta_2 - \alpha_2 \beta_1}{\alpha_2^2}\right)$, was determined by fitting sensitivity data at different values of c_2 using the least squares criterion. The sensitivity data fit in this manner is shown in Figures 21 and 22. These correlations could not be checked for internal consistency because only ratios of parameters can be determined, and they are very sensitive to small perturbations in the parameter values. It is possible, however, to conclude that this method of correlation is adequate to represent the data.

Discussion of Preliminary Results

In this section, the application of the model to single-species fluorescence is discussed in light of the experiments conducted with thioflavin S. The agreement between the experimental results and the

correlational form suggested by the model is excellent. However, the estimates of the parameters are not as good. The parameter, k_2, in equation (31) is predicted to equal $a_{340} + a_{450}$. The value of k_2 found by fitting the experimental data was $0.0172\,\mathrm{cm}^{-1}\mathrm{ppm}^{-1}$. However, $a_{340} + a_{450}$, as measured with a Bausch and Lomb Spectronic® 710 spectrophotometer was $0.0115\mathrm{cm}^{-1}\mathrm{ppm}^{-1}$. Although these two values are of the same order of magnitude, they do differ significantly. Also, the predicted and fitted values of S are $1.33\mathrm{cm}^{-1}$ and $0.412\mathrm{cm}^{-1}$, respectively. This is a much greater discrepancy, but since the value of this parameter is highly dependent on the geometric assumptions that are made, this is expected. Some of the possible reasons for these discrepancies are listed in Table 3.

Below is an elaboration of the causes listed in the table:

(1) Beer's Law doesn't hold – This can easily be determined by measuring the absorbance at different dilutions. This hasn't been done yet. The effect of a nonlinear relationship between absorbance and concentration on the model has not been considered yet.

(2) Systematic error in the length measurement – The measurement of length involved about five separate measurements of constant lengths and one measurement of a variable length. Some of the lengths were added and some subtracted in order to obtain the length that was used. If the constant part of the measurement was in error, there is a systematic error in the lengths used in the model.

(3) Incorrect geometric assumptions made in model – A schematic of the actual arrangement is shown in Figure 2. The 2nd and 3rd levels of approximation are attempts to model this arrangement more precisely. These approximations do not produce an expression in closed form and introduce additional parameters, which are both undesirable qualities. See the **Model Development** section for an explanation of the different levels of approximation.

(4) Detector saturation – A plot of the fluorescence *vs.* concentration data for thioflavin S for infinite path length, shown in Figure 23, suggests that signal saturation is occurring, since the maximum fluorescence signal allowed by the software supplied with the probe is very close to the value of fluorescence at which the curve seems to be leveling off at.

The fact the several fluorescent media components analyzed in the **Model Verification** section have very similar values of maximum fluorescence also suggests detector saturation is occurring. See Figures 19 and 20.

In order to eliminate the possible effects of detector saturation, the experiments with thioflavin S were redone at lower concentrations, corresponding to the linear region of the graph in Figure 23. Results from this analysis *cannot* be compared with the previous results for two reasons: (1) the thioflavin S came from a different lot and (2) the probe had been modified during the time between the two analyses. (Narrowing of the chromatic band width was one of the modifications that was made.) Also, the fluorescence units are different. Determination of model parameters using the low concentration data is very unreliable because the

Table 3: Possible causes for the discrepancy between the predicted and experimentally determined values of S and k_2.

	Cause	Comment or Remedy
(1)	Beer's law does not apply.	Can be tested for by measuring the absorbance at different dilutions. This situation has not been modeled in this paper.
(2)	Systematic error in the length measurement	Sensitivity analysis can be applied to the model.
(3)	Inappropriate geometric assumptions made in the model	More general model can be applied.
(4)	Detector Saturation	Some evidence suggests this is occurring. Measurement of inner filter effects can made in the apparent linear region for the detector.
(5)	Insensitivity of model to values of k_2 and S	Sensitivity analysis can be applied. Depends on range of experiment and possible other causes of nonlinearity.
(6)	Other sources of nonlinearity such as nonmonochromatic light or quenching	The effect of nonmonochromatic light source and/or detector has not been investigated yet. Previously published models of quenching show the same dependence on concentration as in this model for infinite path length.
(7)	Light reflection off of vessel walls or black disc	The apparent value of S would probably decrease, while the apparent value of k_2 would increase.
(8)	Inaccurate absorbance reading due to fluorescence or light-scattering	Need to use a spectrophotometer with the detector a long distance from sample.
(9)	Light-Scattering	This phenomena has been modeled. The effect on the apparent values of k_2 and S will be studied using this model.

relationship is nearly linear in this region, and thus, relatively insensitive to the parameter values. However, the model can be evaluated without introducing other independent sources of nonlinearity by adding a nonfluorescent species that absorbs light at either the excitation or emission wavelength. The exponential constant, k, should increase linearly with the absorbing species concentration. If the coefficient of the absorbing species is equal to the absorptivity, then detector saturation as well as other sources of nonlinearity are possible causes of the discrepancy. Most likely, then, the discrepancy would not have been caused by inappropriate geometric assumptions.

(5) Insensitivity to k_2 and S – At lower concentrations, the equation predicting the fluorescence is insensitive to the value of the exponential constant, k, in equation (32), since absolute experimental errors become relatively large as the signal is lowered. However, at high fluorophore concentrations, the important region in the fluorescence *vs.* path length curves is the short path length region. Experimental uncertainty of the length measurement can cause large random errors in this region, since the fluorescence is most sensitive to length when the path length approaches zero. Only the maximum fluorescence at a particular concentration is known with high certainty. In addition, the parameter, S, has little effect at low concentrations when the fluorescence-concentration relationship is nearly linear.

(6) Other sources of nonlinearity such as nonmonochromatic light or quenching – Other sources of nonlinearity can affect the fluorescence in a such a way as to modify the apparent parameters of the model. The effect of nonmonochromatic light has not been studied, but will be in the near future. Quenching is the radiationless transfer of energy from an excited molecule to an unexcited molecule. The effect is a lowering of the quantum yield by prolonging the lifetime of the excited state. Self-quenching can occur if the fluorescence and absorbance spectra overlap, since a molecule must be capable of absorbing the fluorescent light that the excited molecule would emit since the amount energy transferred is the same. Analyses of quenching for common fluorometer configurations shows the same dependence on concentration as this model does for infinite path lengths. The occurrence of quenching depends of the concentrations of the donor and accepter, and not on light intensity, it is expected that quenching will have no effect on the path length terms. Quenching will be modeled specifically for the current probe configuration.

(7) Light reflection off of vessel walls or black disc– Some of the emitted light could be making its way to the detector by bouncing off of the vessel walls or the black disc positioned to control the path length. In this case, a larger fraction of the emitted light can make its way to the detector. Besides, the fraction is not as strong a function of the path length, L. This will lower the apparent value of the parameter, S, in the factor that determines the fraction of emitted light that can make its way to the detector. However, the effective path length for absorbance of the emitted light will be increased. This would increase the apparent value of

k_2. Thus, the overall effect of light reflecting off of vessel walls is to correct both k_2 and S in the right direction. In order to verify and/or quantify this effect, a different shaped vessel could be used, and/or a different colored disc could be used. This effect would be increased by using a narrower vessel or a lighter colored disc.

(8) Inaccurate absorbance measurement – Absorbance readings can be inaccurate due to the detection of scattered or emitted fluorescent light [52]. When measuring absorbance, one wants to detect all of the scattered light, but none of the fluorescent light. In order to detect as much of the scattered light as possible, the detector should be located as close as possible to the sample vessel. However, in order to detect the least amount of fluorescence, the detector should be located as far from the sample chamber as possible [18]. Thus, the error introduced by the detection of fluorescent light depends on the spectrophotometer configuration. In any event, color filters could be used to filter out light resulting from fluorescence.

(9) Light-scattering – The effect of light-scattering has been modeled. Both the case in which light-scattering is proportional to the fluorophore concentration and the case in which the light-scattering is independent of the fluorophore concentration have been modeled. The effect on the apparent values of S and k_2 will be investigated.

In summary, the form of equation (31) is very appropriate to correlate single-species fluorescence, without any interference due to light-scattering or light absorption by other components. The real test of the model will be the application to multicomponent systems, in which there *is* interference. When the model is applied to this type of system, it will be possible to determine whether or not it is necessary to appply the more general geometric assumptions.

Effect of Environmental Conditions on Model Parameters

Environmental conditions can affect the fluorescence in several manners. If the environment around a fluorophore is changed, this can result in quenching or enhancement of fluorescence. For example, NADH bound to protein is much more fluorescent than free NADH. Also, the absorption spectrum is slightly shifted. Table 4 lists some examples of this effect. As mentioned earlier, the cofactor must be in the reduced form in order for it to be fluorescent. The amount of cofactor in this form is highly dependent on the metabolism of the cells and the availability of energy source and electron accepter, for example, oxygen. Thus, anything that affects a cell's metabolism may have an affect on the cell's fluorescence. A study of the level of pyridine nucleotide coenzymes in microorganisms indicated that the total of all forms of the coenzymes varyed considerably with medium conditions, such as carbon source and oxygen availablity[46]. A third way that environmental conditions can affect the fluorescence measurement is by affecting the light path, either by changing the absorption or light-scattering properties of the medium or changing the light path geometry.

Internal Redox Potential. The logarithm of the ratio of NADH to NAD is proportional to the

Table 4: The effect of protein binding on NADH fluorescence. (DPNH = NADH, TPNH = NADPH) Reproduced from [Udenfriend 1962].

FLUOROMETRIC STUDIES ON DEHYDROGENASE-REDUCED PYRIDINE NUCLEOTIDE COMPLEXES

Enzyme	Coenzyme	Fluorescence		Reference
		Intensity	Direction of spectral shift 200–800 mμ	
Alcohol dehydrogenase (liver)	DPNH	Increased	←	(35)
Alcohol dehydrogenase (yeast)	DPNH	Increased	←	(39)
Lactic dehydrogenase (heart)	DPNH	Increased	←	(22)
Lactic dehydrogenase (liver,	DPNH	Increased	←	(40)
Lactic dehydrogenase (heart and muscle)	DPNH	Increased	←	(38)
Lactic dehydrogenase (heart)	DPNH	Increased	←	(38)
Lactic dehydrogenase (heart)	APDH[a]	Increased	←	(38)
Triosephosphate dehydrogenase	DPNH	Decreased	←	(22)
Glutamic dehydrogenase	DPNH and TPNH	Increased	←	(41)
Malic dehydrogenase	DPNH	Increased	←	(42, 43)
Isocitric dehydrogenase	TPNH	—	←	(44)
Uridine diphosphogalactose-4-epimerase	DPNH	—	←	(45)

[a] APDH = acetylpyridine analog of DPNH.

internal redox potential, E_i, at equilibrium. However, the conditions inside growing cells are not at equilibrium. Instead, chemical reactions within the cells are in a state of quasi-equilibrium or quasi-steady state. In either case, it is probable that $\log\left(\frac{[NADH]}{[NAD]}\right)$ is still a linear function of the internal redox potential, E_i, if it could be measured. In addition, since there is often a constant potential across the cell membrane during balanced exponential growth, the externally measured redox potential would also be a linear function of $\log\left(\frac{[NADH]}{[NAD]}\right)$. Assuming this to be true:

$$\log\left(\frac{[NADH]}{[NAD]}\right) = K \cdot \exp(aE) \tag{41}$$

where E is the externally measured redox potential; K and a are constants.

It is often assumed that the sum of the concentrations of NAD and NADH is a constant. If this is true, the fluorescent yield for cells, $\phi_{X,\lambda\rightarrow\lambda'}$, of equations (20) and (22) would be proportional to $\frac{[NADH]}{[NADH]+[NAD]}$. As a function of [NADH]/[NAD], $\phi_{X,\lambda\rightarrow\lambda'}$ can be expressed as follows:

$$\phi_{X,\lambda\rightarrow\lambda'} = \phi_{X,\lambda\rightarrow\lambda',max} \cdot \left(\frac{[NADH]/[NAD]}{[NADH]/[NAD]+1}\right). \tag{42}$$

The factor, $\phi_{X,\lambda\rightarrow\lambda',max}$ is proportional to the sum of [NADH] and [NAD], whether or not it is constant.

Temperature. Increased temperature results in the increase in the rate of radiationless decay of the excited state, which will decrease the quantum yield. Figure 24 shows the variation of the fluorescence signal with temperature for various fluorescent species.

Increased temperature also results in absorption and emission peak broadening due to the Doppler effect. Most often, this results in a decrease in excitation light absorption and/or fluorescent yield. However, if $\lambda \neq \lambda_{max}$, then the absorbance and/or fluorescent yield may increase with temperature as shown in Figure 25 since the peak may shift or broaden. Native NADH has a negative temperature coefficient of 1.6% per degree [47].

In a separate experiment [83], the fluorescence due to cell mass in a culture of *B. amyloliquefaciens* was shown to be inversely related to the temperature, as detected by oscillations in the fluorescence signal corresponding to simultaneous oscillations in temperature. The sensitivity in this case was $2.6\frac{NFU}{^\circ C}$. See Figure 26.

A change in temperature will have an effect on cellular metabolism, also. This in turn may affect the NADH/NAD ratio within the cells. The temperature will also affect binding constants for NADH-binding proteins. The substrate-protein equilibrium as well as the cofactor-protein equilibrium will affect the fluorescence. There may be other intracellular or extracellular fluorophores or chromophores in equilibrium with less fluorescent or less absorbent species. In general, this equilibrium will be a function of temperature. These absorbent compounds will cause inner-filtering effects.

pH. The sensitivity of the measurement of NADH is slightly dependent upon the pH; and there is

usually a pH corresponding to maximal sensitivity [9]. Figure 27 shows the typical dependence of fluorescence on the pH.

The fluorescence of internal fluorophores is dependent on the internal pH not the external pH. In many instances the internal pH is unaffected by changes in the external pH. However, the fluorescence of internal components will be indirectly affected by the external pH if there are external pH-dependent fluorophores and chromophores. The pH will also affect cellular metabolism, binding constants, and extracellular equilibrium constants just as the temperature does. The quenching ability of accepter molecules may depend on pH. For example, a fiber optic pH probe was developed which takes advantage of the pH-dependence of the quenching of eosin fluorescence by phenol red [38]. The change in the quenching ability of phenol red is reflected by the change in its absorbance spectrum at the emission wavelength of eosin since the accepter molecule must absorb light corresponding to the amount of energy transferred. Whether or not a substance is protonated, in many cases, determines if it is fluorescent. Figure 28 lists a number of compounds that are fluorescent in only one of these two states.

The pH also affects the redox potential across cell membranes. Thus, the redox state of the NADH:NAD couple may be affected.

Bubbles. Bubbles will tend to decrease the absorbance terms and light-scattering terms due to medium components including cells while increasing the light-scattering due to bubbles. Thus, light-scattering terms will increase relative to the the concentration coefficients as the aeration rate is increased.

Cell Size. The most obvious is the effect on light-scattering. Actually, the size of clumps of cells is more important in some cases. Of course, cell size is a reflection of cellular metabolism and growth conditions, so there will probably be a combination of effects on the fluorescence.

Other Fluorophores. Since there are quite a number of biological fluorophores, (See table 5 for a partial list.) it is likely that other cellular or medium components will have significant fluorescence measurable to the probe, even though the emission and excitation peaks are separated. According to table 5, histamine, L-DOPA, vitamin A, and folic acid have emission and excitation peaks near those of NADH, and it is expected (if their concentrations are high enough) that these compounds would contribute significantly to the fluorescence probe tuned for NADH. However, F_{420} and a commercial preparation of riboflavin were both found to have significant fluorescence as measured by the FluroMeasure^{TM} probe even though their emission and excitation peaks are far removed from those of NADH. Many complex medium components such as yeast extract, peptone, dried bakers' yeast, and casein are significantly fluorescent as measured by the probe. The fluorescent components have not been identified yet (probably flavins or riboflavins). If the level of these components remains constant, the multi-component fluorescence model can be used to estimate the concentration of a particular component of variable concentration. Otherwise, the concentration of these components must be estimated by other means. See **Linearization of Fluorescence Signal** section.

Experiments will be conducted to see how the parameters of the model vary with changes in temperature, pH, and bubble concentration.

Linearization of Fluorescence Signal

If $A_{\lambda,\lambda'} = \frac{\left[1-\exp\left(-L\left[\sum_{i=1}^{N}\left(a_{i,\lambda}+a_{i,\lambda'}\right)c_i+S\right]\right)\right]}{\sum_{i=1}^{N}\left(a_{i,\lambda}c_i+a_{i,\lambda'}c_i\right)+S}$ can be measured independently, then the normalized fluorescence, $\frac{\Delta F}{A_{\lambda,\lambda'}I_\lambda}$, is a linear function of the fluorophore concentrations:

$$\frac{\Delta F}{A_{\lambda,\lambda'}I_\lambda} = \sum_{i=1}^{N}\phi_i a_{i,\lambda}c_i. \tag{43}$$

The filtering due to absorbance and light-scattering due to particulate matter at both wavelengths can be measured with spectrophotometers set to the respective wavelengths. The contribution to S due to light-divergence can be estimated as shown previously. However, it is more desirable to obtain this value experimentally so that all other factors can be accounted for. The light-scattering due to bubbles, on the other hand, presents a problem. If the absorbances at the excitation and emission wavelengths are measured outside the fermentor, the light-scattering due to bubbles will not be measured. One solution to this problem is to estimate the light-scattering due to bubbles as a function of the aeration rate. Another solution is to measure the fluorescence outside the fermentor in a sampling loop, after degassing the liquid in the sampling loop. The possible problem of a sampling delay must be considered in this case. A third solution involves measuring the absorbance inside the fermentor, including light-scattering due to bubbles, using fiber optics. Care needs to be taken so that the optical probes devices are sufficiently separated inside the fermentor such that stray light from one probe doesn't interfere with measurement of the other probe(s). Using this coupling procedure, fluorophore concentration can be estimated even when the optical parameters of the system are not held constant.

It is readily apparent that if more than one fluorophore concentration is unknown, it is impossible to estimate one of the fluorophore concentrations from a single-excitation, single-emission signal. Since the fluorescence spectra will vary in shape and in intensity, it is possible to deduce several fluorophore concentrations from a series of fluorescence measurements at different excitation and/or emission frequencies, provided that the relationship between fluorophore concentration and fluorescence can be decoupled. The linearization technique discussed above, would be useful for this, since the fluorescence divided by the absorption factor is of a linear combination of the fluorophore concentrations. Thus, it is suggested that multi-channel fluorescent measurement be coupled with appropriate absorption measurements in order to linearize the fluorophore-fluorescence relationship.

Thus, for more than one emission-excitation wavelength pair:

$$\begin{bmatrix} (\Delta \dot{F}/AI)_1 \\ \vdots \\ (\Delta F/AI)_j \\ \vdots \\ (\Delta F/AI)_n \end{bmatrix} = \begin{bmatrix} \phi_{11}a_{11} & \cdots & \cdots & \cdots & \phi_{1n}a_{1n} \\ \vdots & \ddots & & & \vdots \\ \vdots & & \phi_{ij}a_{ij} & & \vdots \\ \vdots & & & \ddots & \vdots \\ \phi_{n1}a_{n1} & \cdots & \cdots & \cdots & \phi_{nn}a_{nn} \end{bmatrix} \begin{bmatrix} c_1 \\ \vdots \\ c_i \\ \vdots \\ c_n \end{bmatrix} \tag{44}$$

where:

$(\Delta F/AI)_j$ is the normalized fluorescence signal for the ith component using the jth pair of emission and excitation wavelengths.

a_{ij} is the absorbance of component i at the excitation wavelength using the jth pair of emission and excitation wavelengths.

ϕ_{ij} is the fluorescence yield for component i using the jth pair of emission and excitation wavelengths.

c_i is the concentration of component i

If this $(n \times n)$ matrix is well-conditioned, then the fluorophore concentration can be deduced, provided the fluorescent yield and absorbance for each fluorophore is known at each excitation-emission light wavelength pair. If more than n measurements are made, the matrix becomes $(m \times n)$, where m is the number of measurements. In this case, the matrix may be rank-deficient and singular value decomposition should be used to determine the best values for the fluorophore concentrations.

If multi-channel fluorescence is employed as a measurement, there are other fluorophores beside NAD(P)H which will be of interest. Very recently, the fluorescence characteristics of *Staphylococcus epidermidis, Pseudomonas fluorescens, Enterobacter cloacae, Escherichia coli,* and *Bacillus subtilis* were measured [20]. Emission spectra for several excitation wavelengths were measured, and the excitation spectra for several emission wavelengths were also measured. Finally, the lifetimes of the fluorescence at several pairs of excitation and emission wavelengths were measured. Table 5 lists some important biological substances that are fluorescent.

Table 5: Other Biological Fluorophores

Fluorophore	*Maximum Wavelength*	
	Excitation	Emission
NAD(P)H (reduced form only)	340	460
F_{420} (oxidized form only)	425	472
Flavins (oxidized form only) [74]	450	535
Riboflavins	445	520
Tyrosine	275	303
Tryptophan	287	348
Phenylalanine	260	282
Histamine	340	480
p-Aminobenzoic acid	294	345
Vitamin B_{12}	275	305
Vitamin A	372	510
Folic Acid	365	450
Estrogens	285	325
ATD, ADP, etc.	272	380
Serotonin	295	330
L-DOPA	345	410
Antibiotics	Var.	Var.

Conclusions and Recommendations

1. The form of the simple model presented here can be used to correlate the fluorescence of a one-component solution with the fluorophore concentration as well as path length.
2. The fluorophore-fluorescence relationship is inherently nonlinear. This is primarily due to inner-filtering and geometric effects which are accounted for in the model.
3. The classical analysis is not appropriate for an open-ended sample because the "monitoring efficiency" is a function of the position in the sample .
4. The variation of the sensitivity of the fluorescence signal to the fluorophore concentration can be correlated with the concentration of a background component, using the model.
5. Concentration terms are additive, so that composite properties can be used. Also, deconvolution of multicomponent fluorescence is easier.
6. Parameter estimation needs to be improved, possibly by broadening the model to consider divergent light-source, light-scattering, re-emitted light, and non-monochromatic light-source and detector.
7. By measuring the sample's absorbance at both the excitation and emission wavelengths, an absorbance correction can be used to linearize the relationship between fluorophore concentration and fluorescence.
8. Only one fluorophore concentration can vary, when using only one excitation and emission wavelength pair. When more than one vary, deconvolution is required. Time-decay data as well as the fluorescence at other wavelength pairs can be used for deconvolution of the signal.

Nomenclature

$a_{i,\lambda}$; $a_{i,\lambda'}$ Exctinction coefficient of species i at the excitation and emission wavelegths, respectively.

c_i; c Concentration of species i.

$-(dI_\lambda(x))_i$ Amount of excitation light absorbed by component i with a differential slice.

$(dE_\lambda(x))_i$ Amount of light emitted by component i with a differential slice.

$E_{\lambda'}(x)$ Intensity of emission light as a function of the distance from the probe tip.

ΔF Measured fluorescence intensity.

F_{max}; k Exponential parameters used to correlate the fluorescence with path length.

F_0 Background fluorescence.

$f(x, R)$ Monitoring efficiency at point x, as a function of the detector radius.

$I_\lambda(0)$ Intensity of light-source as it enters the sample solution.

$I_\lambda(x)$ Intensity of excitation light as a function of the distance from the probe tip.

$I_{\lambda'}(x)$ Intensity of emission light as a function of the distance from the probe tip.

l_2 Distance emitted light must travel in order to reach the detecter.

L Total path length in the sample.

N Number of species in a multi-component mixture.

NADH; NAD Reduced and oxidized forms of the cofactor nicotinamide adenine dinucleotide, respectively.

OD_λ; OD'_λ Absorbance of the sample at the excitation and emission wavelengths, respectively.

R Effective radius of the detector surface.

S Geometric parameter used to approximate the monitoring efficiency as a function of the position in the sample.

x Distance from the probe tip.

X Cell mass concentration. (Subscript, X, denotes celluar properties.)

α; α'; β; β' Parameters used to correlate multicomponent fluorescnce data.

λ; λ' Wavelengths of the excitation and detected emission light, respectively.

$\phi_{i,\lambda\rightarrow\lambda'}$; $\phi_{\lambda\rightarrow\lambda'}$ Fluorescent yield – Ratio of the amount of the light emitted at wavelegths detectable by the probe, around λ', to the amount of light absorbed at λ. Differs from the "quantum yield", because only the emitted light at wavelegth, λ' is considered in this case.

φ' Cone angle which defines the monitoring efficiency at a any position in the sample.

φ; φ_{max} Cone angle describing the spreading of the excitation light.

θ' Circular angle of emitted light.

References

[1] **Appellof, C.J. and E.R. Davidson.** 1981. Strategies for analyzing data from video fluorometric monitoring of liquid chromatographic effluents. *Anal. Chem.* **53**: 2053-2056.

[2] **Armiger, W.B., J.R. Forro, J.F. Lee, G. MacMichael, and R. Mutharasan.** Sept. 1986. On-line measurement of hybridoma growth by culture fluorescence. in press.

[3] **Armiger, W.B., J.F. Forro, L.M. Montalvo, J.F. Lee, and D.W. Zabriskie.** 1986. The interpretation of on-line process measurements of intracellular NADH in fermentation processes. *Chem. Eng. Commun.* **45**: 197-206.

[4] **Atkins, P.W.** 1978. Physical Chemistry. W. H. Freeman and Company, San Francisco, CA.

[5] **Beull, M.V. and R.E. Hansen.** 1957. Spectrophotometry in the Far Ultraviolet. *Science* **126**: 842.

[6] **Beyeler, W., A. Einsele, and A. Fiechter.** 1981. On-line measurement of culture fluorescence: method and application. *Eur. J. Appl. Microbiol. Biotechnol.* **13**: 10-14.

[7] **Beyeler, W.** 1982. Fluoreszenz-messungen in bioreaktoren -eine neue moeglichkeit zur kontrolle mikrobieller prozesse. *Chem-Ing-Tech* **54**, 5:498.

[8] **Binot, R.A., H.P. Naveau, and E.-J. Nyns.** 1981. Methanogenic potential activity of mixed liquors: fluorimetric monitoring. *Biotechnol. Lett.* **3**(11) 623-628.

[9] **BioChemTechnology.** FluroFacts. Malvern,PA.

[10] **BioChemTechnology.** 1987. The FluroMeasure® System User's Manual. Malvern, PA.

[11] **Bowen, E.J., F. Wokes.** 1953. Fluorescence of Solutions. Longmans, Green and Co, New York, NY.

[12] **Chance, B..** 1954. Spectrophotometry of intracellular respiratory pigments. *Science* **120**: 767-775.

[13] **Chance, B., R.W. Estabrook, and A Ghosh.** 1964. Damped sinusoidal oscillations of cytoplasmic reduced pyridine nucleotide in yeast cells.*Biochemistry* **54**: 1244-1251.

[14] **Chasin, L.A. and J. Szulmajster.** 1969. Enzymes of dipicolinic acid biosynthesis in *Bacillus subtilis.* in Campbell, L.L, ed. Spores IV. American Society for Microbiology, Bethesda, MD.

[15] **Chasin, L.A. and J. Szulmajster.** 1967. Biosynthesis of dipicolinic acid in *Bacillus subtilis. Biochem. Biophys. Res. Commun.* **29**(5): 648-654.

[16] **Christmann, D.R., S.R. Crouch, and A. Timnick.** 1983. Precision and accuracy of absorption-corrected molecular fluorescence measurements by the cell shift method. *Anal. Chem.* **53**: 2040-2044.

[17] **Christmann, D.R., S.R. Crouch, and A. Timnick.** 1981. Automated instrument for absorption-corrected molecular fluorescence measurements by the cell shift method. *Anal. Chem.* **53**: 276-280.

[18] **Clayton, R.K.** 1972. Light and Living Matter, Volume 1: The Physical Part. McGraw-Hill Book Company, New York, NY.

[19] **Codoñer, A., I.S. Monzó, F. Tomás, and R. Valero.** 1986. Spectroscopic study of intermolecular complexes between FAD and some β-carboline derivatives. *Spectrochimica Acta* **42A**(7): 765-769.

[20] **Dalterio, R.A., W.H. Nelson, D. Britt, J.F. Sperry, J.F. Tanguay, and S.L. Suib.** 1987. The steady-state and decay characteristics of primary fluorescence from live bacteria. *Appl. Spectroscopy* **41** 234-241.

[21] **Delafontaine, M.J., H.P. Naveau, and E.J. Nyns.** Fluorimetric monitoring of methanogenesis in anaerobic digestors. *Biotechnol. Lett.* **1**(2): 71-74.

[22] **Doddema, H.J. and G.D. Vogels.** 1978. Improved identification of methanogenic bacteria by fluorescence microscopy. *Appl. Environ. Microbiol.* **36**(5): 752-754.

[23] **Duysens, L. N. M. and J. Amesz.** 1957. Fluorescence spectrophotometry of reduced phosphopyridine nucleotide in intact cells in the near-ultraviolet and visible region. *Biochim. Biophys. Acta* **24**: 19-26.

[24] **Einsele, D.L. Ristroph, and A.E. Humphrey.** 1978. Mixing times and glucose uptake measurement with a fluorometer. *Biotechnol. Bioeng.* **20**: 1487-1492.

[25] **Einsele, D.L. Ristroph, and A.E. Humphrey.** 1978. Substrate uptake mechanisms for yeast cells: a new approach utilizing a fluorometer. *Eur. J. Appl. Microbiol.* **6**: 335-339.

[26] **Ellis, D.W.** 1966. Luminescence instrumentation and experimental details. in Hercules, D.M., ed. Fluorescence and Phosphorescence Analysis: Principles and Applications. Interscience Publishers, New York, NY.

[27] **Estabrook, R.W. and P.K. Maitra.** 1962, A fluorimetric method for the quantitative microanalysis of adenine and pyridine nucleotides. *Anal. Biochem.* **3**: 369-382.

[28] **Galeotti, T., G.D.V. vanRossum D.H. Mayer, and B. Chance.** 1970. On the fluorescence of nad(p)h in whole-cell preparations of tumours and normal tissues. *Eur. J. Biochem.* **17**: 485-496.

[29] **Goodwin, C.D. W.X. Balcavage, and J.R. Mattoon.** 1974. Energy metabolism in *Saccharomyces cerevisiae*: effect of progressive starvation on respiration and pyridine nucleotide reduction linked to ethanol oxidation in intact cells. *Arch. Biochem. Biophys.* **165**: 413-420.

[30] **Gottschalk, G.** 1985. Bacterial Metabolism, 2nd Ed. Springer-Verlag, New York, NY.

[31] **Gschwend, K., W. Beyeler, and A. Fiechter.** 1983. Detection of reactor nonhomogeneities by measuring culture fluorescence. *Biotechnol. Bioeng.* **25**: 2789-2793.

[32] **Guilbault, G.G.** 1967. Fluorescence: Theory, Instrumentation, and Practice. Marcel Dekker, Inc., New York, NY.

[33] **Gunn, A.H.** 1963. Introduction to Fluorimetry. Electronic Instruments Ltd., Richmond, UK.

[34] **Haddock, B. A. and C. W. Jones.** 1977. Bacterial respiration. *Bact. Rev.* **41**: 47-99.

[35] **Harrison, D.E.F. and B. Chance.**1970. Fluorimetric technique for monitoring changes in the level of reduced nicotinamide nucleotides in continuous cultures of microorganisms. *Appl. Microbiol.***19**(3): 446-450.

[36] **Hirschlaff, E.** 1938. Fluorescence and Phosphofluorescence. Meuthen & Co., Ltd., London, UK.

[37] **Ingold Electrodes, Inc.** Ingold Fluorosensor^{TM}: Theory and Applications. Wilmington, MA.

[38] **Jordan, D.M. and D.R. Walt.** 1987. Physiological pH fiber-optic chemical sensor based on energy transfer. *Anal. Chem.* **59**: 437-349.

[39] **Kaplan, N.O.** 1960. The pyridine coenzymes. in Boyer, P.D., H. Lardy, and K. Myrbäck, eds. The Enzymes, volume 3: Prosthetic Groups and Cofactors (Part B), 2nd ed. Academic Press, New York, NY.

[40] **Knoester, J. and J.E. Van Himbergen.** 1987. Monte Carlo simulations on concentration self-quenching by statistical traps. *J. Chem. Phys.* **86**(6): 3577-3582.

[41] **Knorr, F.J. and J.M. Harris.** 1981. Resolution of Multicomponent Fluorescence Spectra by an Emission Wavelength-Decay Time Data Matrix. *Anal. Chem.* **53**: 272-276.

[42] **Kohen, E., C. Kohen, B. Thorell, and D. Schachtschabel.** 1975. Multisite analysis of metabolic transients is single living cells by multichannel microfluorometry. *Mikrochimica Acta* **I**: 223-236.

[43] **Kuhlmann, W., H.-D. Meyer, K.H. Bellgardt, and K. Schügerl.** 1984. On-line analysis of yeast growth and alcohol production. *J. Biotechnol.* **1**: 171-185.

[44] **Leese, R.A. and E.L. Wehry.** 1978. Corrections for inner-filter effects in fluorescence quenching measurements via right-angle and front-surface illumination. *Anal. Chem.* **50**(8): 1193-1197.

[45] **Lipton, P.** 1973. Effects of membrane depolarization on nicotinamide nucleotide fluorescence in brain slices. *Biochem J.* **136**: 999-1009.

[46] **London, J. and M. Knight.** 1966. Concentrations of nicotinamide nucleotide coenzymes in micro-organisms. *J. Gen. Microbiol.* **44**: 241-254.

[47] **Lowry, O.H. and J.V. Passonneau.** 1972. A Flexible System of Enzymatic Analysis. Academic Press, New York, NY.

[48] **Luong, J.H.T. and D.J. Carrier.** 1986. On-line measurement of culture fluorescence during cultivation of *Methylomonas mucosa*. *Appl. Microbiol. Biotechnol.* **24**: 65-70.

[49] **MacBride, W.R., J.A. Magee, W.B. Armiger, and D.W. Zabriskie.** 1986. Optical Apparatus and Method for Measuring the Characteristics of Materials by Their Fluorescence. *U.S. Patent 4,577,110.*

[50] **Maple, J.R. and E.L. Wehry.** 1981. Matrix isolation site selection in fluorescence spectrometry of polar derivatives of polycyclic aromatic hydrocarbons. *Anal. Chem.* **53**: 266-271.

[51] **Mayer, D.H., J.R. Williamson, and V. Legallais.** 1969. A sensitive filter fluorometer for metabolite assays. *Chem. Instrumentation.* **1**(4): 383-389.

[52] **Mehler, A.H., B. Bloom, M.E. Ahrendt, and D. Steven, Jr.** 1957. Artifact in spectrophotometry caused by fluorescence. *Science* **126**: 1285-1286.

[53] **Meyer, C. and W. Beyeler.** 1984. Control strategies for continuous bioprocess based on biological activities. *Biotechnol. Bioeng.* **26**: 916-925.

[54] **Meyer, H.-D., W. Beyeler, and A. Fietcher.** 1984. Experiences with the on-line measurement of culture fluorescence during cultivation of *Bacillus subtilis*, *Escherichia coli* and *Sporotrichum thermophile*. *J. Biotechnol.* **1**: 341-349.

[55] **Mink, R.W. and P.R. Dugan,** 1977. Tentative identification of methanogenic bacteria by fluorescence microscopy. *Appl. Environ. Microbiol.* **33**(3): 713-717.

[56] **Nimmo, H.G.** 1984. Control of *Escherichia coli* isocitrate dehydrogenase: an example of protein phosphorylation in prokaryote. *Trends Biol. Science* **9**: 475-478.

[57] **Parker, C.A. and W.J. Barnes** 1957. Some experiments with spectrofluorimeters and filter fluorimeters. *Analyst* **82**: 606-618.

[58] **Peña, A., G. Cinco, A. Gómez-Puyou, and M. Tuena.** 1972. Effect of the pH of the incubation medium on glycolysis and respiration in *Saccharomyces cerevisiae*. *Arch. Biochem. Biophys.* **153**: 413-425.

[59] **Polakis, E.S. and W. Bartley** 1966. Changes in the intracellular concentration of adenosine phosphates and nicotinamide nucleotides during the aerobic growth cycles of yeast on different carbon sources. *Biochem J.* **99**: 521-533.

[60] **Reardon, K.F., Th. Scheper, and J.E. Bailey.** 1986. In *situ* fluorescence monitoring of immobilized *Clostridium Acetobutylicum*. *Biotechnol. Lett.* **8**: 817-822.

[61] **Reuter, B.W., T. Egeler, H. Schneckenburger, and S.M. Schoberth.** 1986. In vivo measurement of F_{420} fluorescence in cultures of *Methanobacterium thermoautotrophicum*. *J. Biotechnol.* **4**: 325-332.

[62] **Ristroph, D.L., C.M. Watteeuw, W.B. Armiger, and A.E. Humphrey.** 1977. Experience in the use of culture fluorescence for monitoring fermentations. *J. Ferment. Technol.* **55**: 599-608.

[63] **Rollefson, G.K. and H. W. Dodgen.** 1944. The dependence of the intensity of fluorescence on the composition of a fluorescing solution. *J. Phys. Chem.* **21**(3): 107-111.

[64] **Sanwal, B.D.** 1970. Allosteric controls of amphibolic pathways in bacteria. *Bact. Rev.* **34**: 20-39.

[65] **Scheper, T., A. Gebauer, W. Kuhlmann, H.-D. Meyer, and K. Schueger.** 1984. Messung der kulturfluoreszenz aur fermentationskontrolle. *DECHEMA-Monographien 95*, Verlag Chemie, Weinheim, BRD.

[66] **Scheper, Th., A. Gebauer, A. Sauerbrei, A. Niehoff, and K. Schügerl.** 1984. Measurement of biological parameters during fermentation processes. *Anal. Chem Acta* **163**: 111-118.

[67] **Scheper, Th.** 1985. Messung zellinterner und zellexterner parameter zur Fermentationskontrolle. Dissertation, University of Hannover, BRD.

[68] **Scheper, Th. and K. Schuegerl.** 1986. Culture fluorescence studies on aerobic continuous cultures of *Saccharomyces cerevisiae*. *Appl. Microbiol. Biotechnol.* **23**: 440-444.

[69] **Scheper, Th. and K. Schügerl.** 1986. Characterization of bioreactores by in-situ fluorometry. *J. Biotechnol.* **3**: 221-229.

[70] **Scheper, Th., W. Lorenz, W. Schmidt, and K. Schügerl.** 1986. Measurement of culture fluorescence during the cultivation of *Penicillium chrysogenum* and *Zymomonas mobilis*. *J. Biotechnol.* **3**: 231-238.

[71] **Scheper, Th., A. Gebauer, and K. Schügerl.** 1987. Monitoring of NADH-dependent culture fluorescence during the cultivation of *Escherichia coli*. *Chem. Eng. J.* **34**: B7-B12.

[72] **Schneckenburger, H., B.W. Reuter, and S.M. Schoberth.** 1984. Time-resolved microfluorescence for measuring coenzyme F_{420} in *Methanobacterium thermoautotrophicum*. *FEMS Microbiol. Lett.* **22**: 205-208.

[73] **Schneckenburger, H. and B.W. Reuter.** 1984. Time-resolved fluorescence microscopy for measuring specific coenzymes in methanogenic bacteria. *Anal. Chem Acta* **163**: 249-255.

[74] **Schneckenburger, H. B.W. Reuter, and S.M. Schoberth.** 1985. Fluorescence techniques in biotechnology. *Trends Biotechnol.* **3**(10): 257-261.

[75] **Schwartz, A.C. and R. Schäfer.** 1973. New amino acids, and heterocyclic compounds participating in the Stickland Reaction of *Clostridium sticklandii*. *Arch. Mikrobiol.* **93**: 267-276.

[76] **Srinivas, S.P. and R. Mutharasan.** 1987. Culture fluorescence characteristics and its metabolic significance in batch cultures of *Clostridium acetobutylicum*. *Biotechnol. Lett.* **9**(2): 139-142.

[77] **Street, K.W. and A. Singh.** 1985. Fluorescence signal enhancement using double pass cell configurations. *Anal. Lett.* **18(A4)**: 529-542.

[78] **Street, K.W., Jr.** 1987. Fluorescence inner filtering in double-pass configurations: part 2. validity of assumptions for primary inner filtering diagnosis. *Analyst* **112**: 167-169.

[79] **Takebe, I. and K. Kitahara** 1963. Levels of nicotinamide nucleotide coenzymes in lactic acid bacteria. *J. Gen. Appl. Microbiol.* **9**(4): 31-40.

[80] **Udenfriend, S.** 1962. Fluorescence Assay in Biology and Medicine. Academic Press, New York, NY.

[81] **Wang, D.I.C., C.I. Cooney, A.I. Demain, P. Dunnill, A.E. Humphrey, and M.D. Lilly.** 1979. Fermentation Kinetics. in Fermentaion and Enzyme Technology. John Wiley & Sons, Inc., New York, NY.

[82] **Watteeuw, C.M., W.B. Armiger, D.L. Ristroph, and A.E. Humphrey.** 1979. Production of single cell protein from ethanol by fed-batch process. *Biotechnol. Bioeng.* **21**: 1221-1237.

[83] **Yoo, Y.J. and M.B. Simmons** 1985-1986. Unpublished data.

[84] **Zabriskie, D. W.** 1976. "Real-time Estimation of Aerobic Batch Fermentation Biomass Concentration by Component Balancing and Culture Fluorescence," Ph.D. dissertation, University of Pennsylvania, Dept. of Chem. and Biochem. Eng., Philadelphia, PA.

[85] **Zabriskie, D. W. and A. E. Humphrey.** 1978. Estimation of fermentation biomass concentration by measuring culture fluorescence. *Appl. Environ. Microbiol.* **36**(2): 337-343.

[86] **Zabriskie, D. W.** 1979. Use of culture fluorescence for monitoring of fermentation systems *Biotechn Bioeng Symp 9*, 117-123.

Figure 1: Some important branch points in cellular metabolism involving NAD(P)H.

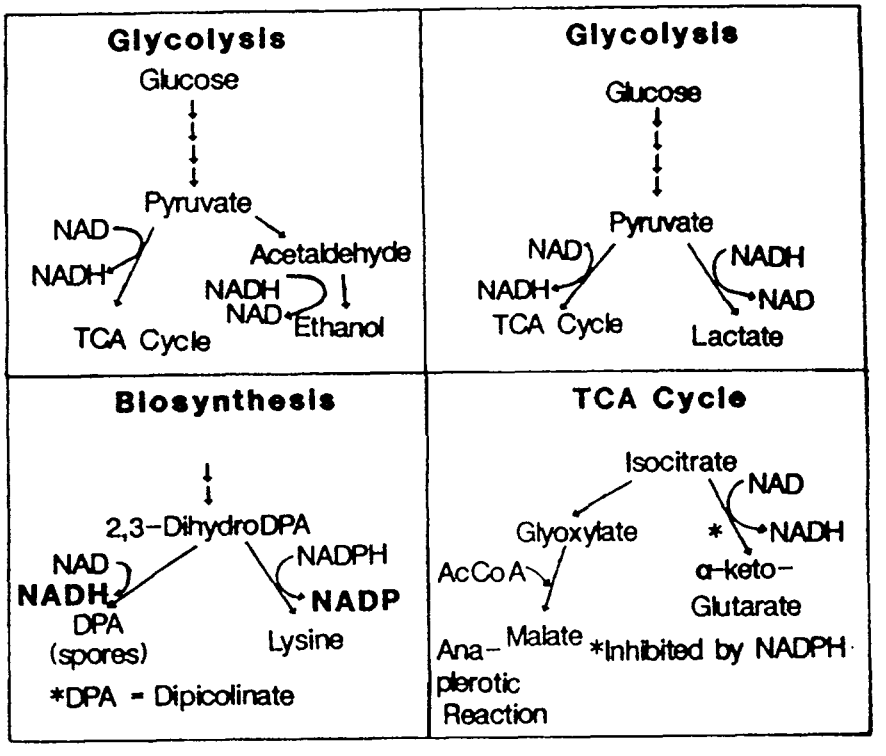

Figure 2: Schematic of actual probe configuration. Reproduced from [MacBride et al. 1986].

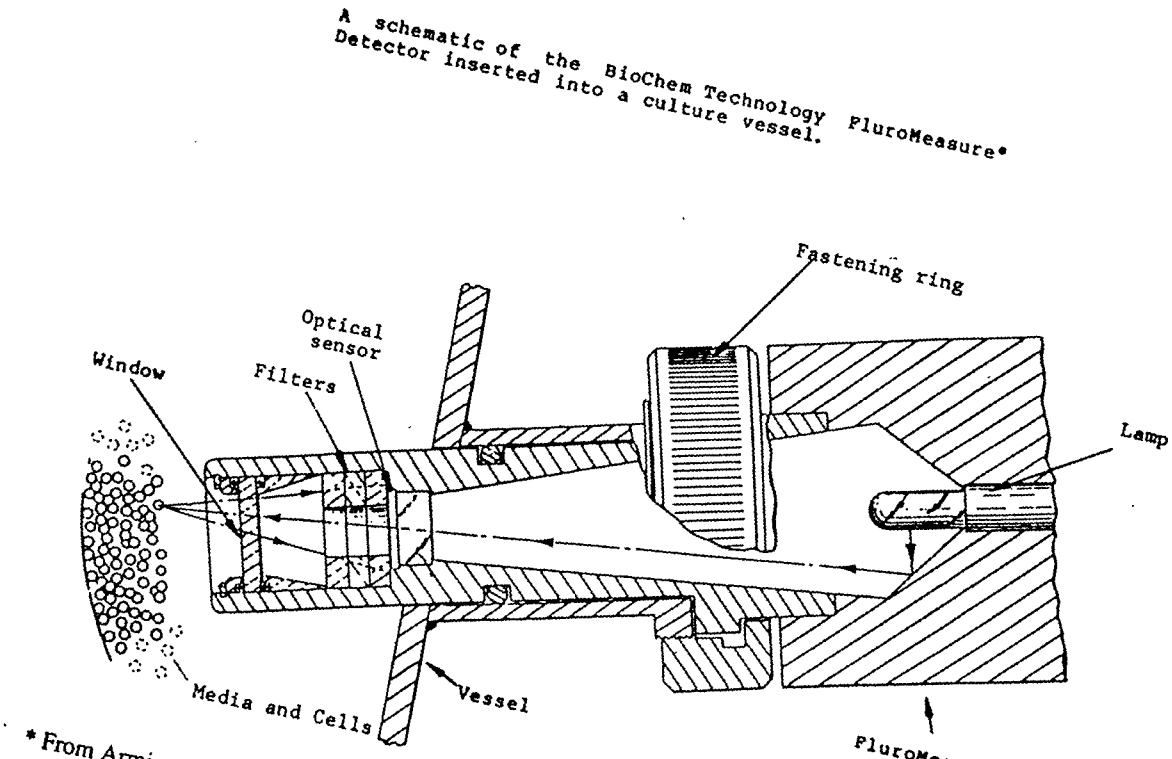

* From Armiger, W.B. *et al.*, paper presented at *British Laboratory Week*, Olympia, London, UK, 1986.

Figure 3: Amount of total light emitted that is aimed back at the detector surface as defined by the cone angle, φ_2' or the distance from the probe, x, and the radius, R, of the effective detector surface.

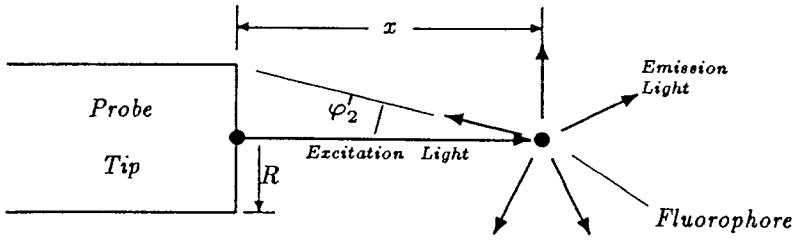

Figure 4: Approximation of $f(x, R)$ with a single exponential parameter, S. The values, $S = 1.0\,\mathrm{cm}^{-1}$ and $S = 1.2\,\mathrm{cm}^{-1}$ are used for approximations shown in Figures 5 and 6, respectively.

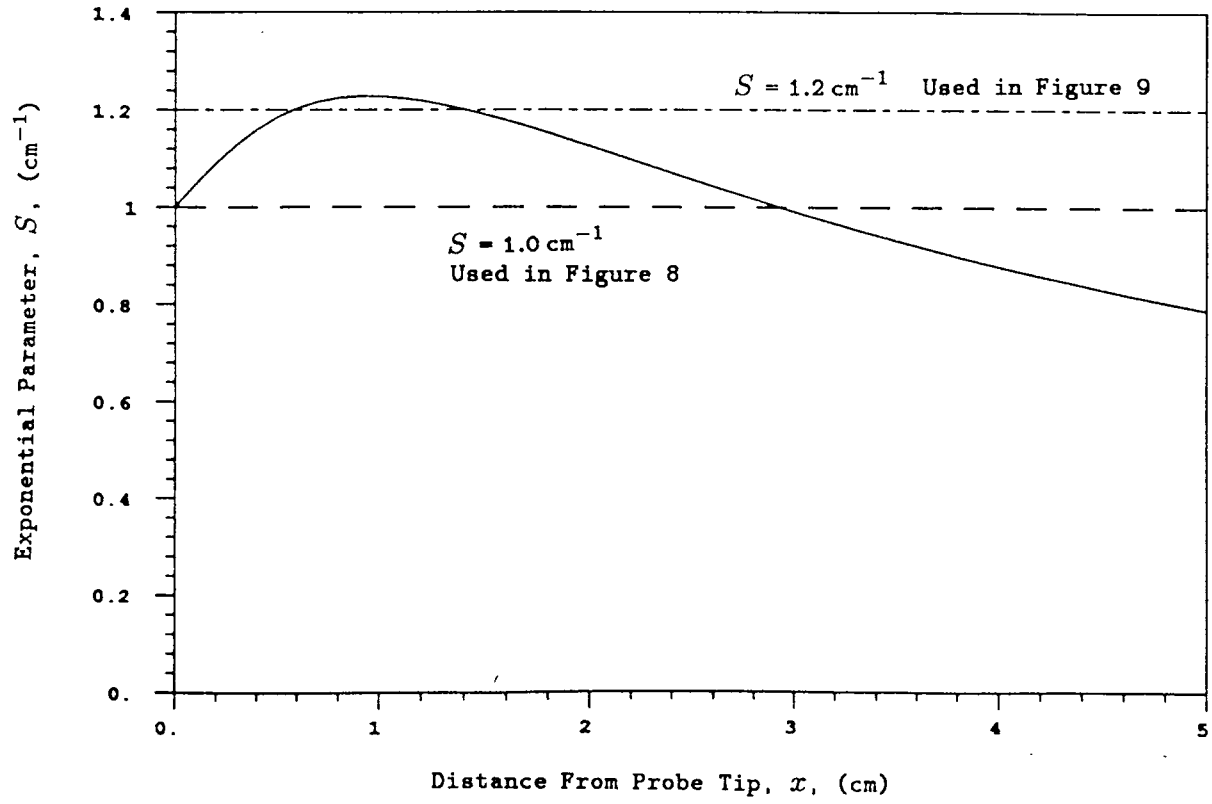

Figure 5: The effect of approximating the factor, $f(x,R) = \left(1 - \frac{x}{\sqrt{x^2+R^2}}\right)$ with $f(x,S) = e^{-xS}$. This is a comparison of equations (15) and (17b), using $N = 1$; $\frac{1}{2}I_\lambda(0) = 200$; $\phi_{1,\lambda\to\lambda'} = 0.0556$; $a_{1,\lambda} = 0.09$; $a_{1,\lambda'} = 0.01$; and $R = 1.0\,\mathrm{cm}^{-1}$. In equation (17b), $S = 1/R = 1.0\,\mathrm{cm}^{-1}$ is used.

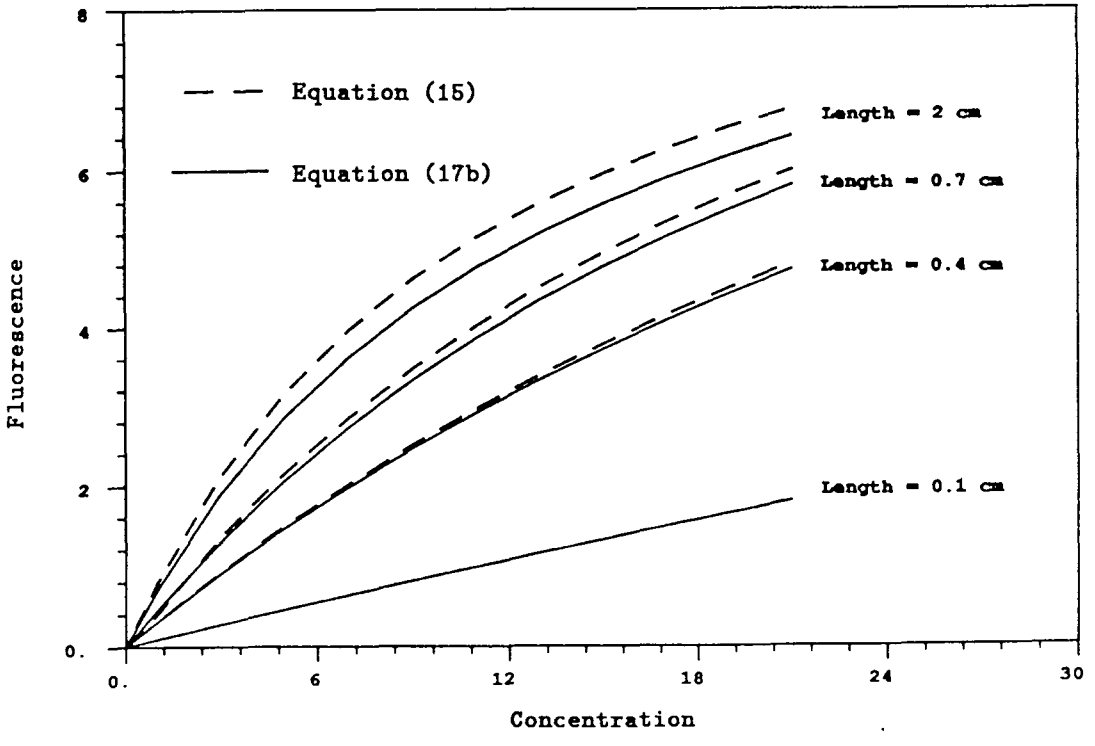

Figure 6: The effect of approximating the factor, $f(x,R) = \left(1 - \frac{x}{\sqrt{x^2+R^2}}\right)$ with $f(x,S) = e^{-xS}$. This is a comparison of equations (15) and (17b), using $N = 1$; $\frac{1}{2}I_\lambda(0) = 200$; $\phi_{1,\lambda\to\lambda'} = 0.0556$; $a_{1,\lambda} = 0.09$; $a_{1,\lambda'} = 0.01$; and $R = 1.0\,\mathrm{cm}^{-1}$. In equation (17b), $S = 1/R = 1.2\,\mathrm{cm}^{-1}$ is used.

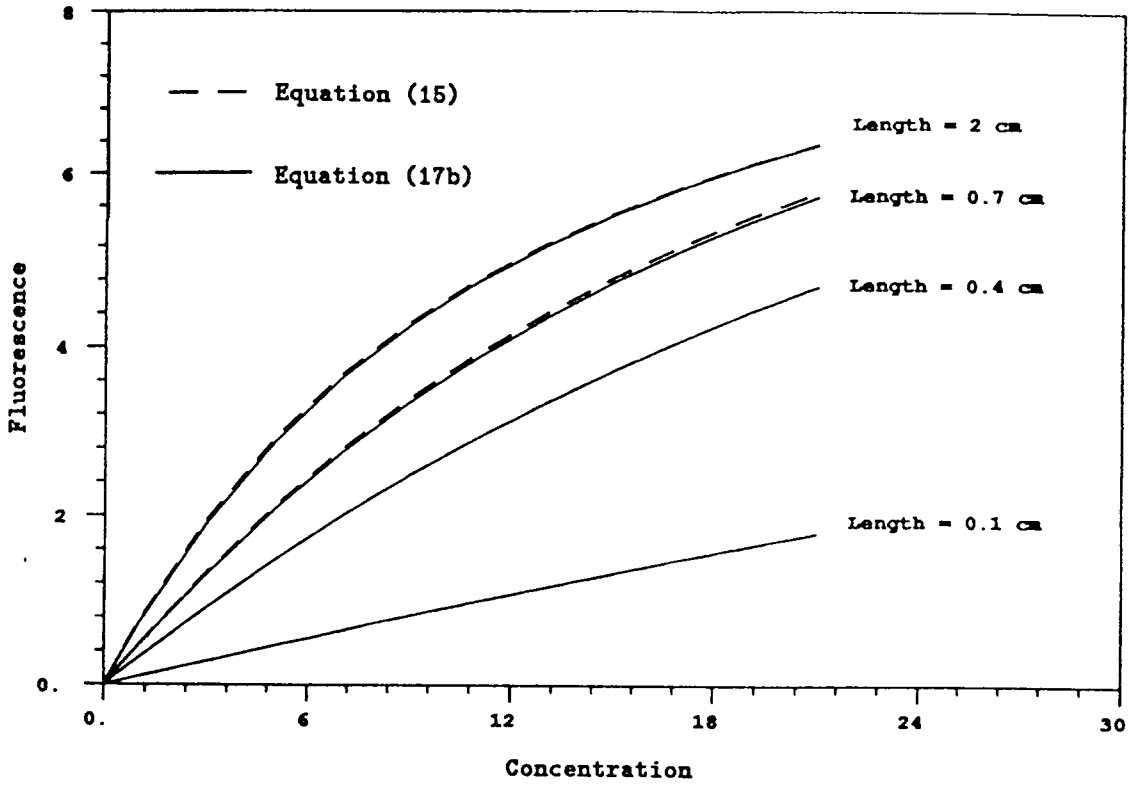

Figure 7: The effect of finite path length on the predicted fluorescence signal. Comparison of equations (18) and (17) using $N = 1$; $\frac{1}{2}I_\lambda(0) = 200$; $\phi_{1,\lambda\to\lambda'} = 0.0556$; $a_{1,\lambda} = 0.09$; $a_{1,\lambda'} = 0.01$; and $S = 1/R = 1.2\,\mathrm{cm}^{-1}$.

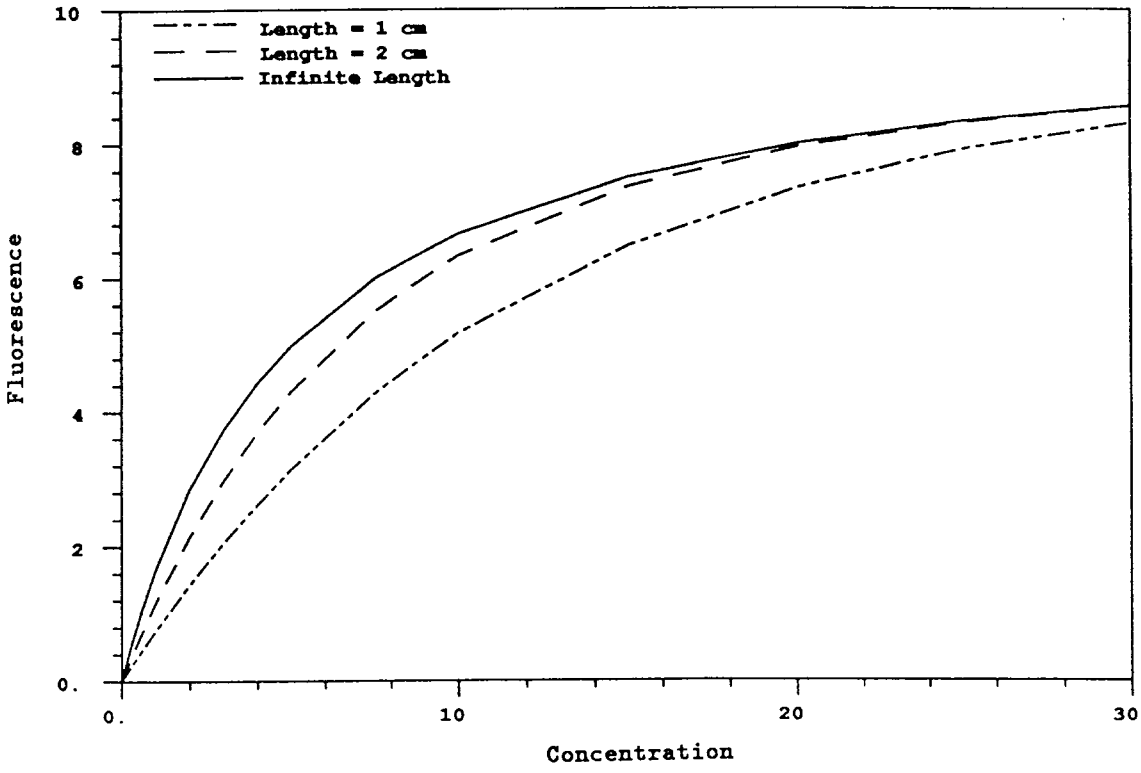

Figure 8: Error in fluorophore concentration estimation caused by a drift in the background fluorescence. It is assumed that there are only 2 components present. For both components, $a_{1,\lambda} = 0.09$ and $a_{1,\lambda'} = 0.01$. The parameter, S, was set to $1.0\,\mathrm{cm}^{-1}$, and $\frac{1}{2}I_\lambda(0)$ was set to 200. The fluorescent yield for component 1, $\phi_{1,\lambda\to\lambda'}$, was set to 0.0556. The cases in which $\phi_2 = \phi_1$, $\phi_2 = 10\phi_1$, and $\phi_2 = 0.1\phi_1$ were considered. The concentration of the second component was chosen such that its fluorescence in the absence of of component 1 would be equal to the fluorescence of a solution containing only component 1.

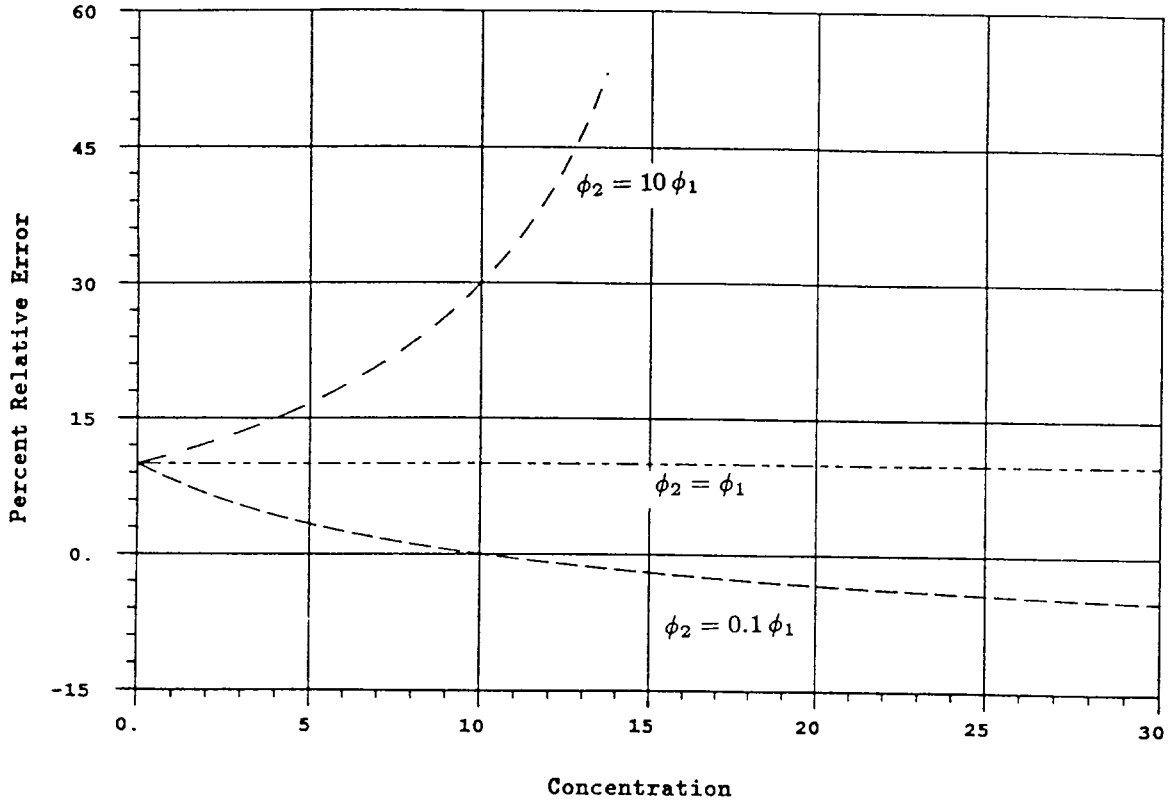

Figure 9: Spreading of the excitation light over the cone angle, φ_{max}, as modeled at the second level of approximation.

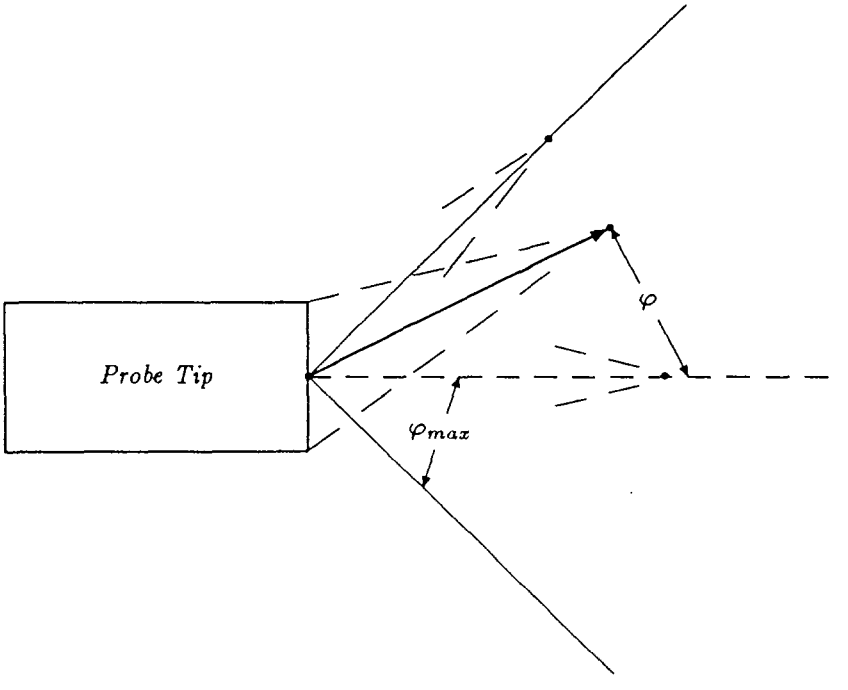

Figure 10: Experimental setup used to verify the model

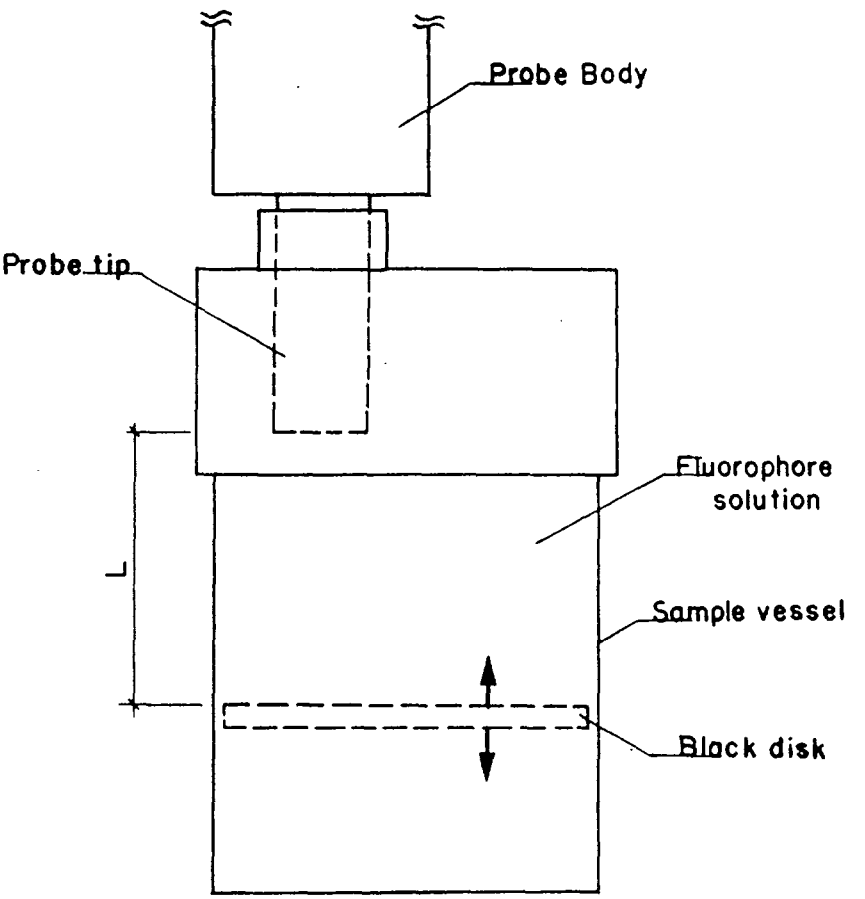

Figure 11: Model verification using thioflavin S. The fluorescence signal is correlated as a function of the path length, according to equation (32), for each of the four fluorophore concentrations listed below. The curves were evaluated using equation (32) with parameters as shown below.

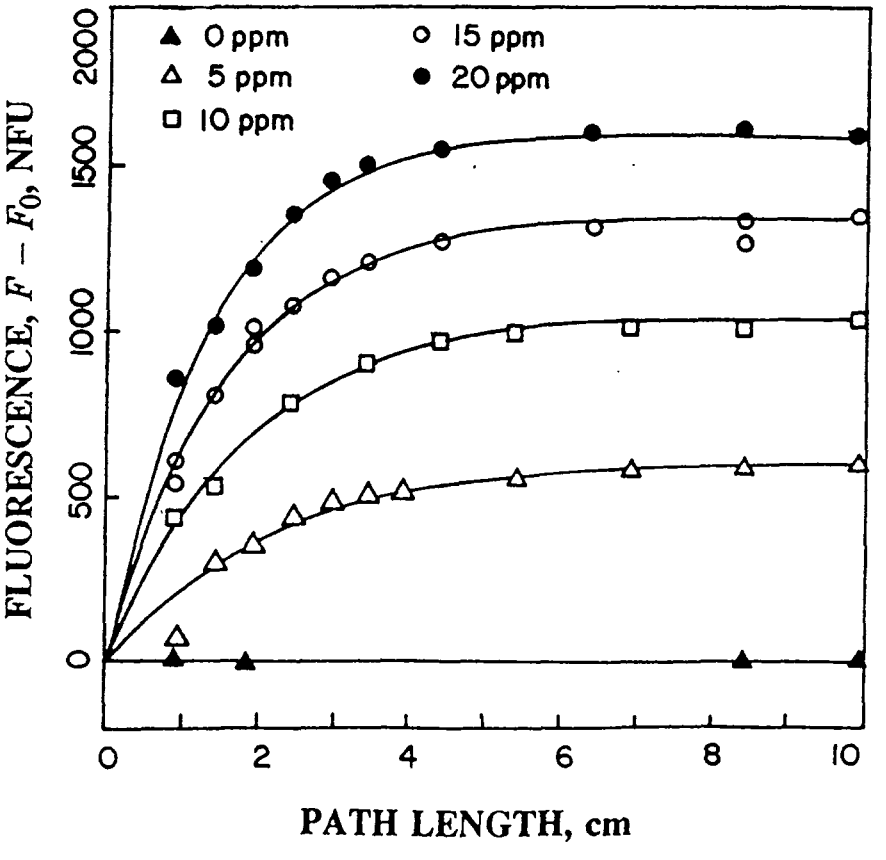

$$\Delta F = F_{max}[1 - \exp(-kL)]$$

c	F_{max}	k
5 ppm	605.1	0.4794
10 ppm	1040.1	0.5704
15 ppm	1343.1	0.6720
20 ppm	1595.2	0.7748

Figure 12: Correlation of the exponential constant, k, with the concentration of thioflavin S, corresponding to the data in Figure 11.

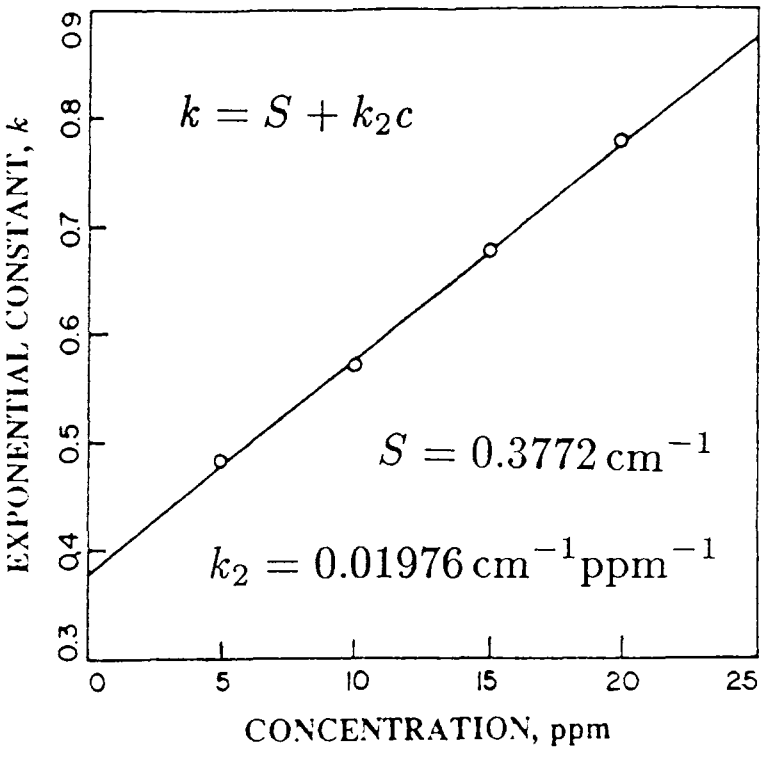

Figure 13: Correlation of the exponential constant, F_{max}, with the concentration of thioflavin S, corresponding to the data in Figure 11.

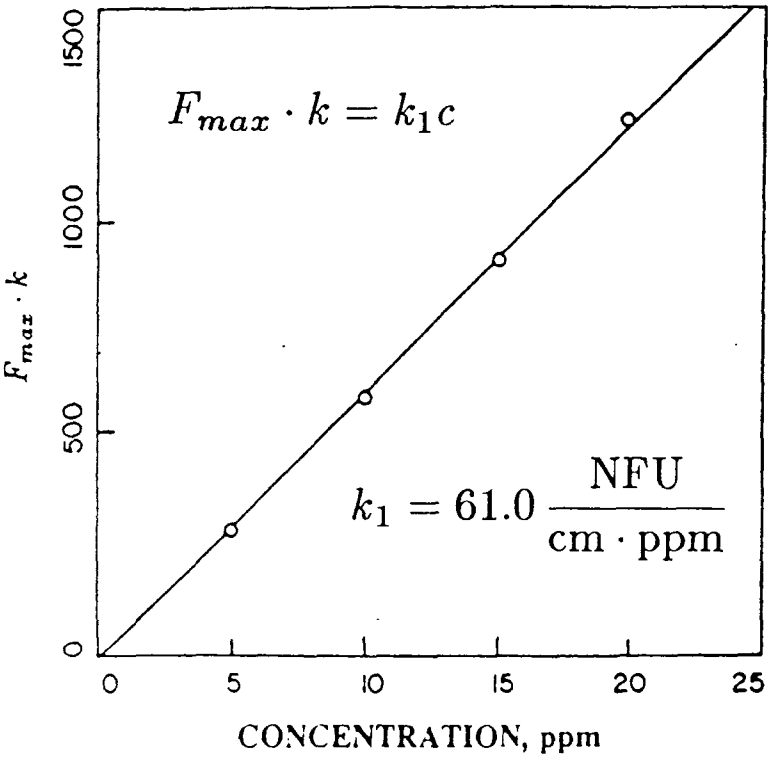

Figure 14: Correlation of the fluorescence signal due to thioflavin S with the fluorophore concentration and path length according to equation (31). The data is the same as in Figure 11. The curves are a result of evaluating equation (31) with $S = 0.412\,\mathrm{cm}^{-1}$, $k_1 = 60.3\,\frac{\mathrm{NFU}}{\mathrm{cm\ ppm}}$, and $k_2 = 0.0172\,\mathrm{cm}^{-1}\mathrm{ppm}^{-1}$.

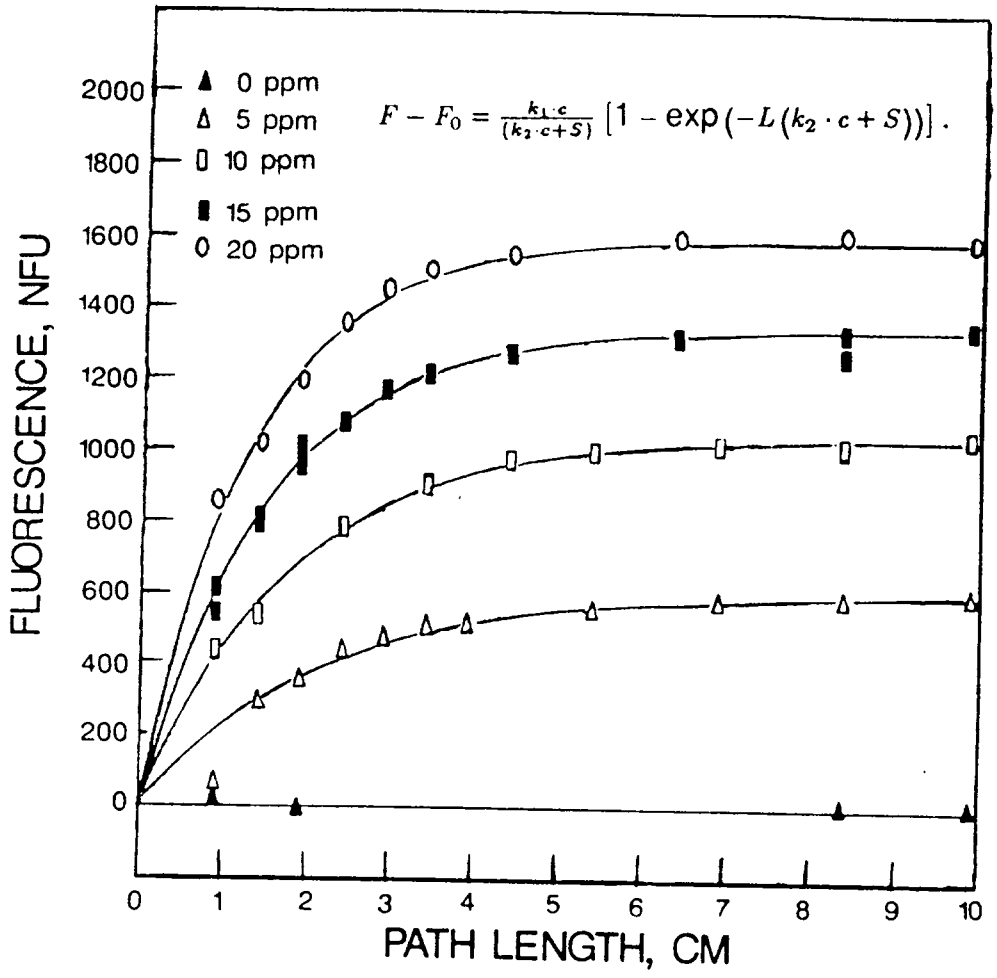

Figure 15: Model verification using thioflavin S at lower concentrations. The fluorescence signal is correlated as a function of the path length, according to equation (32), for each of the four fluorophore concentrations. The numbers used to represent the data points indicate the thioflavin S concentrations in ppm. The curves were evaluated using equation (32) with parameters as shown below.

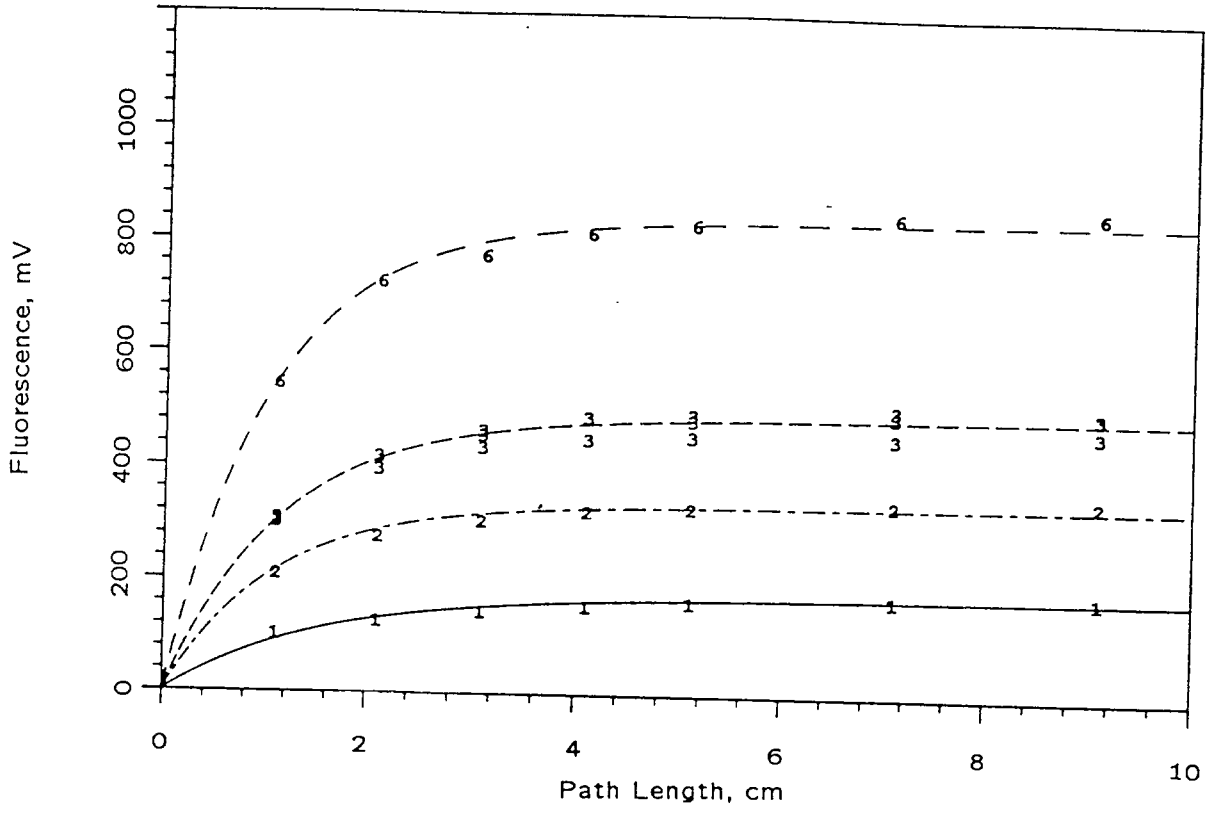

$$\Delta F = F_{max}[1 - \exp(-kL)]$$

c	F_{max}	k
1 ppm	174	0.6793
2 ppm	335	0.9354
3 ppm	490	0.8719
6 ppm	838	0.9622

Figure 16: Correlation of the exponential constant, k, with the concentration of thioflavin S, corresponding to the data in Figure 15.

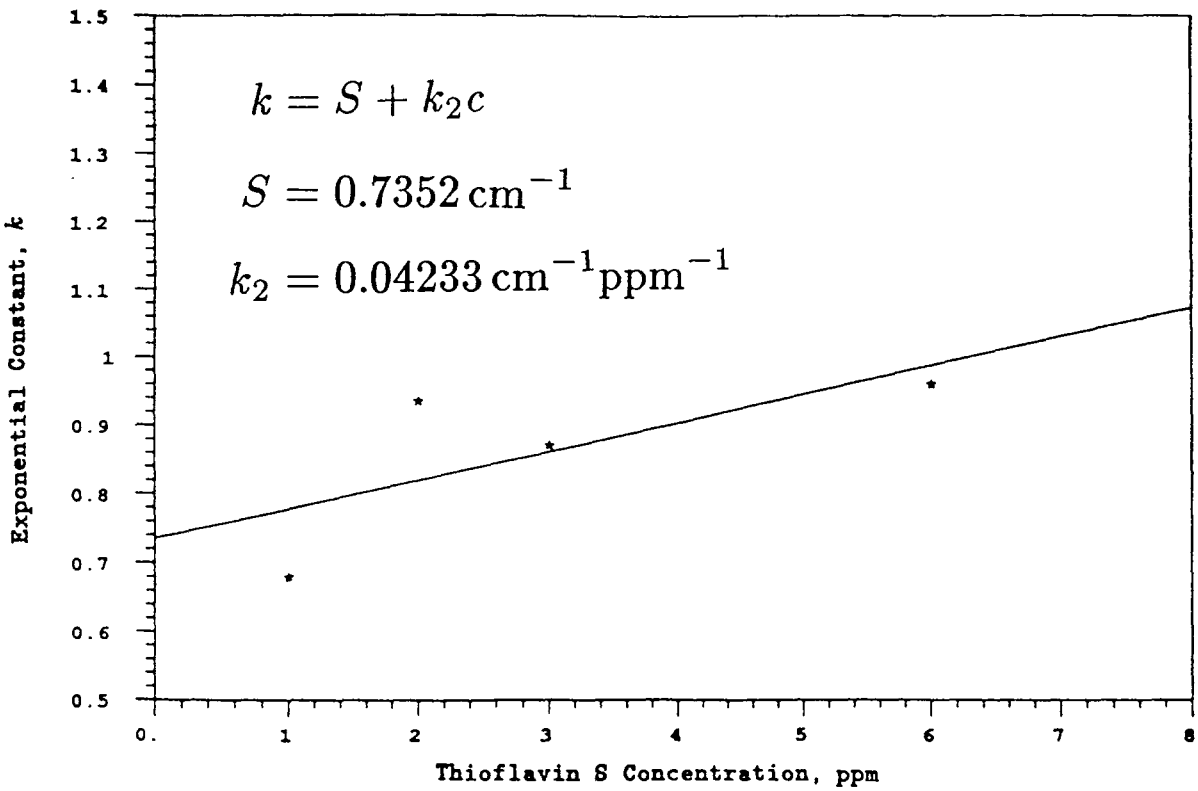

Figure 17: Correlation of the exponential constant, F_{max}, with the concentration of thioflavin S, corresponding to the data in Figure 15.

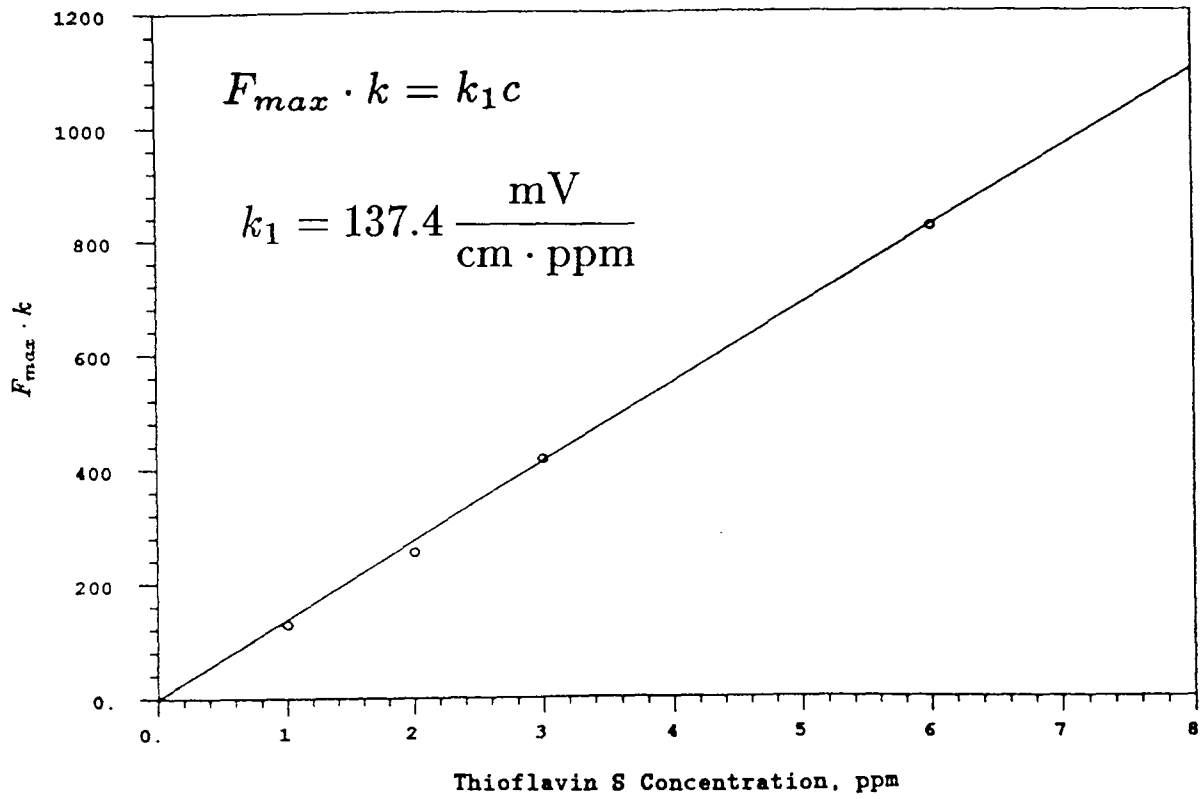

Figure 18: Correlation of the fluorescence signal due to thioflavin S with the fluorophore concentration and path length according to equation (31). The data is the same as in Figure 15. The numbers representing the data points indicate the thioflavin concentration. The curves are a result of evaluating equation (31) with $S = 0.7352\,\mathrm{cm}^{-1}$, $k_1 = 137.4\,\frac{\mathrm{mV}}{\mathrm{cm\ ppm}}$, and $k_2 = 0.04233\,\mathrm{cm}^{-1}\mathrm{ppm}^{-1}$.

$$\Delta F = \frac{k_1 \cdot c}{(k_2 \cdot c + S)}\left[1 - \exp\left(-L\,(k_2 \cdot c + S)\right)\right]$$

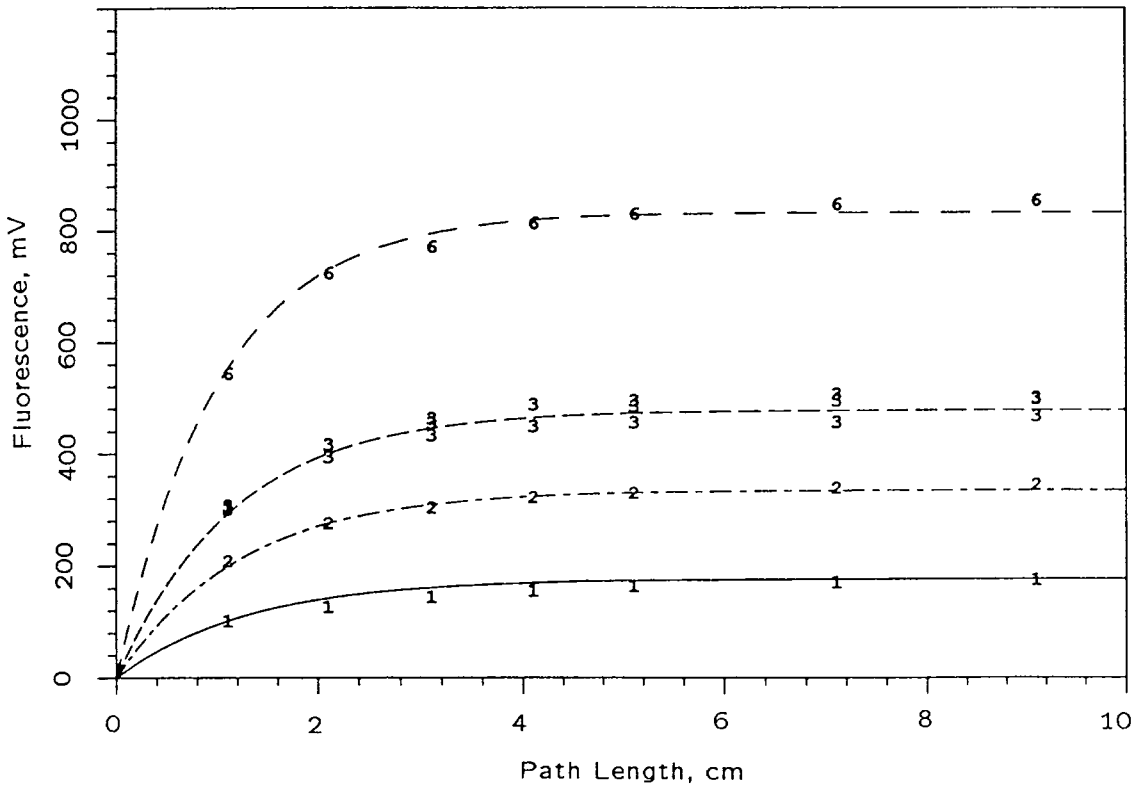

Figure 19: Correlation of media background fluorescence.

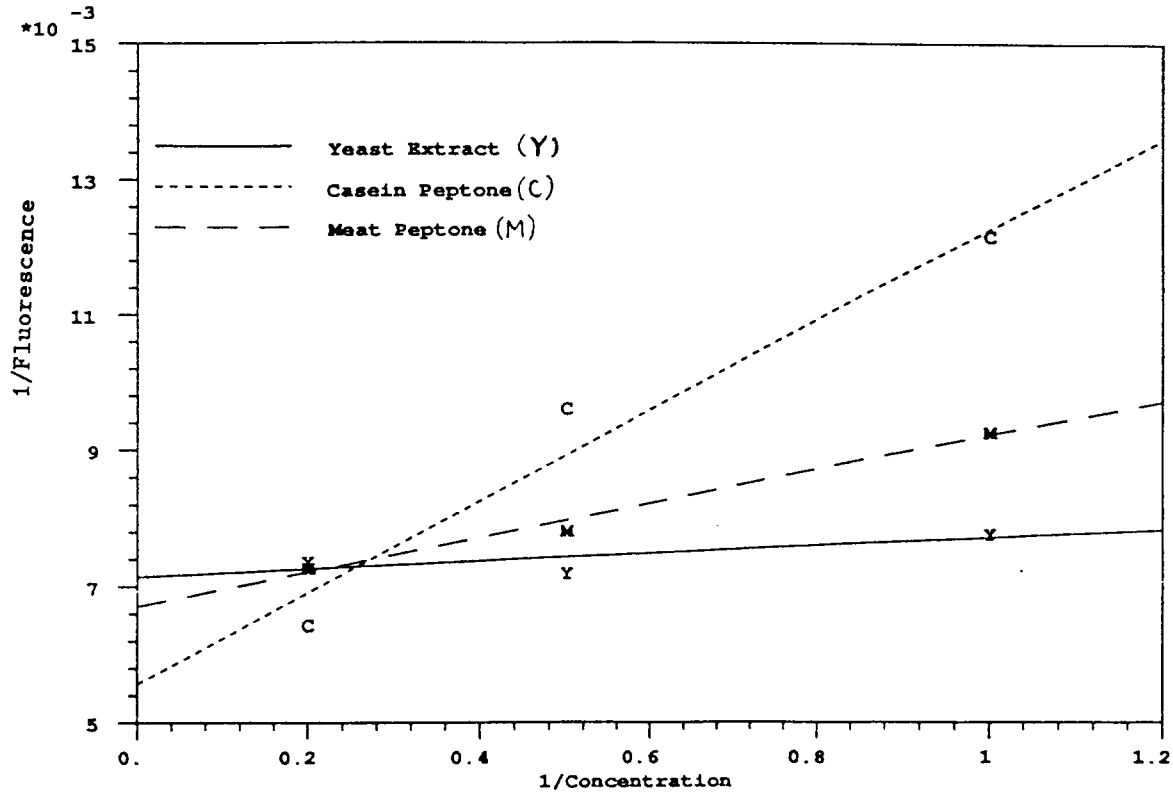

Figure 20: Correlation of media background fluorescence.

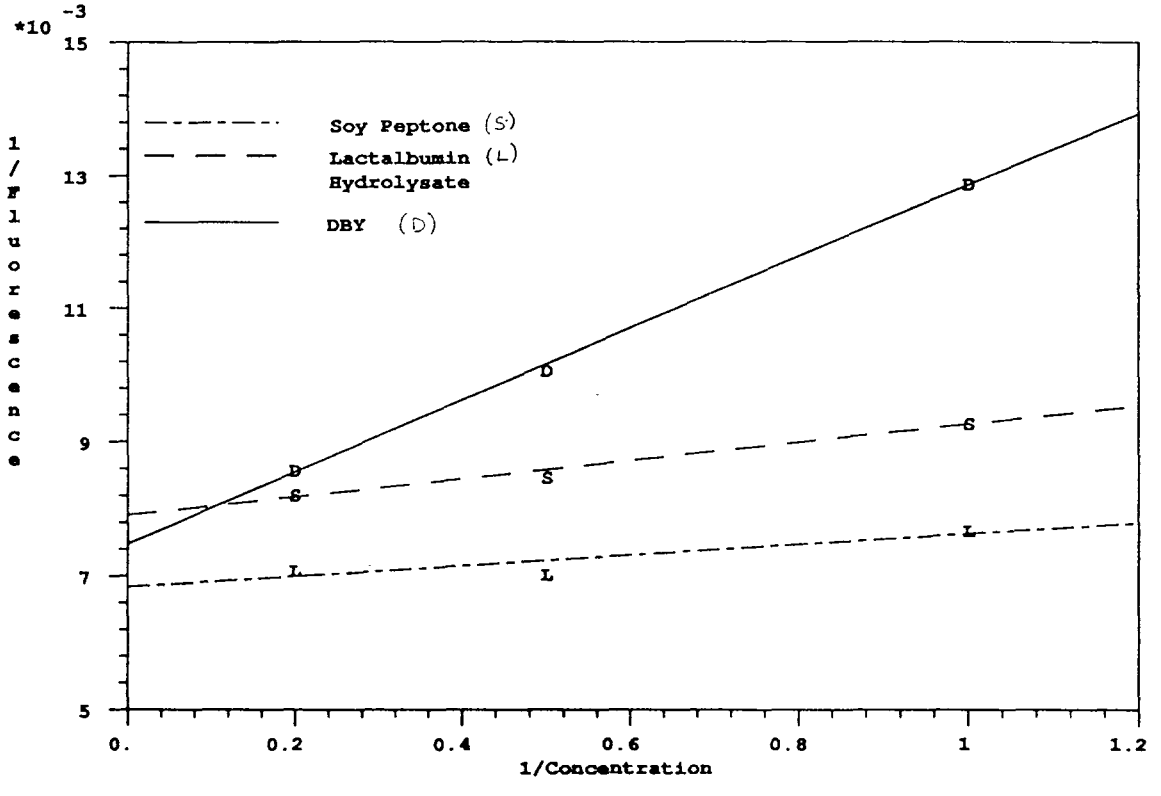

Figure 21: Correlation of fluorescence sensitivity to NADH as a function of background fluorophore concentration using equation (40).

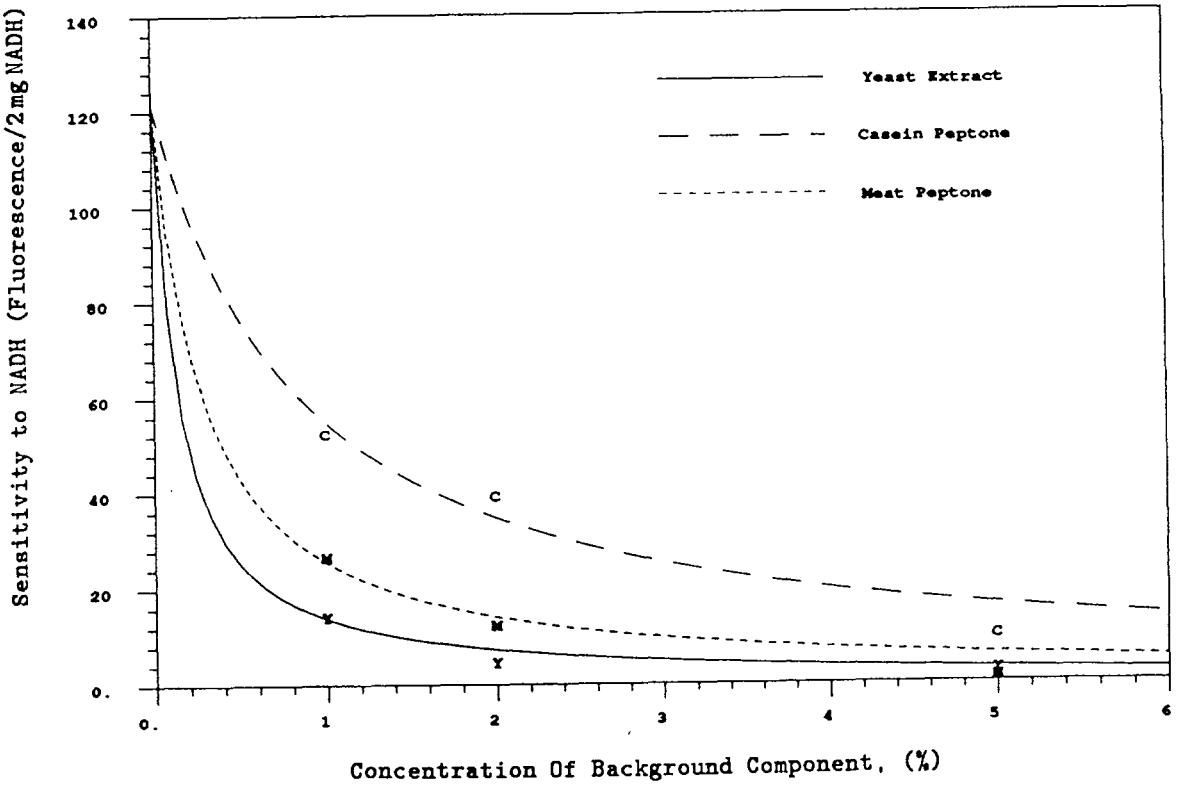

Figure 22: Correlation of fluorescence sensitivity to NADH as a function of background fluorophore concentration using equation (40).

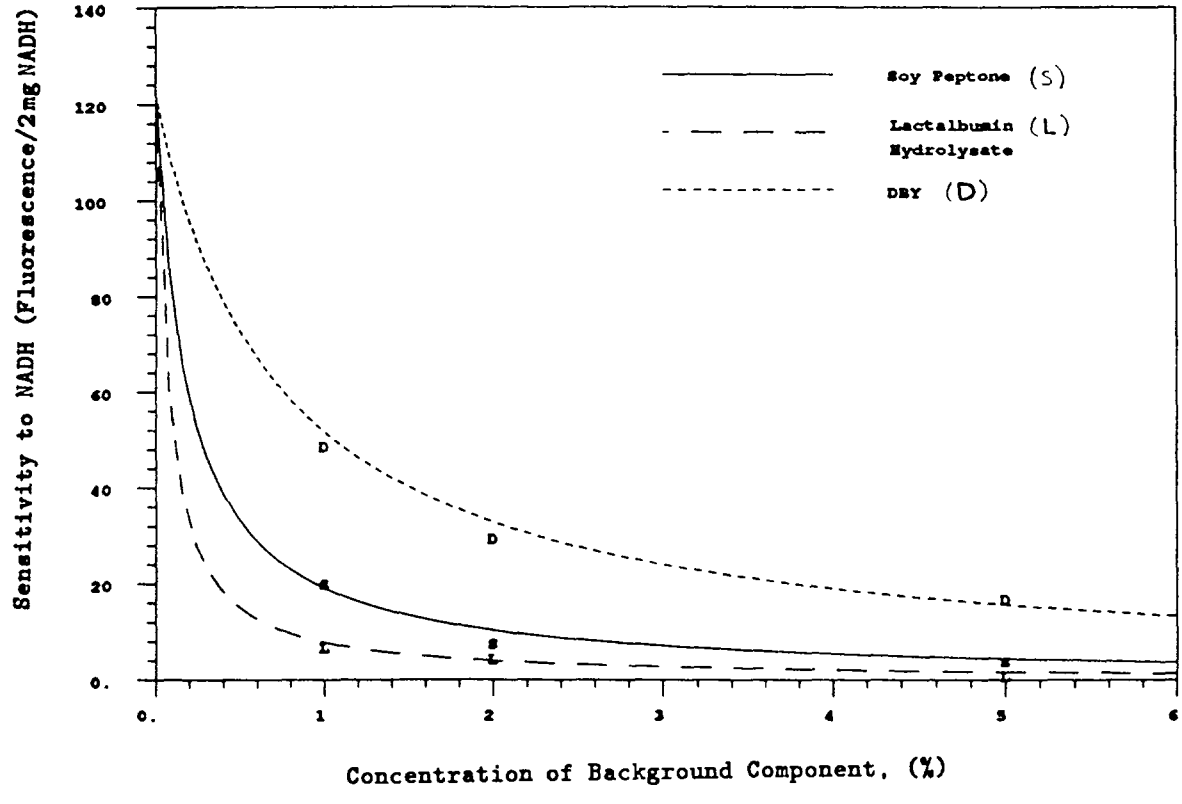

Figure 23: Full scale dependence of fluorescence on thioflavin S concentration at infinite path length.

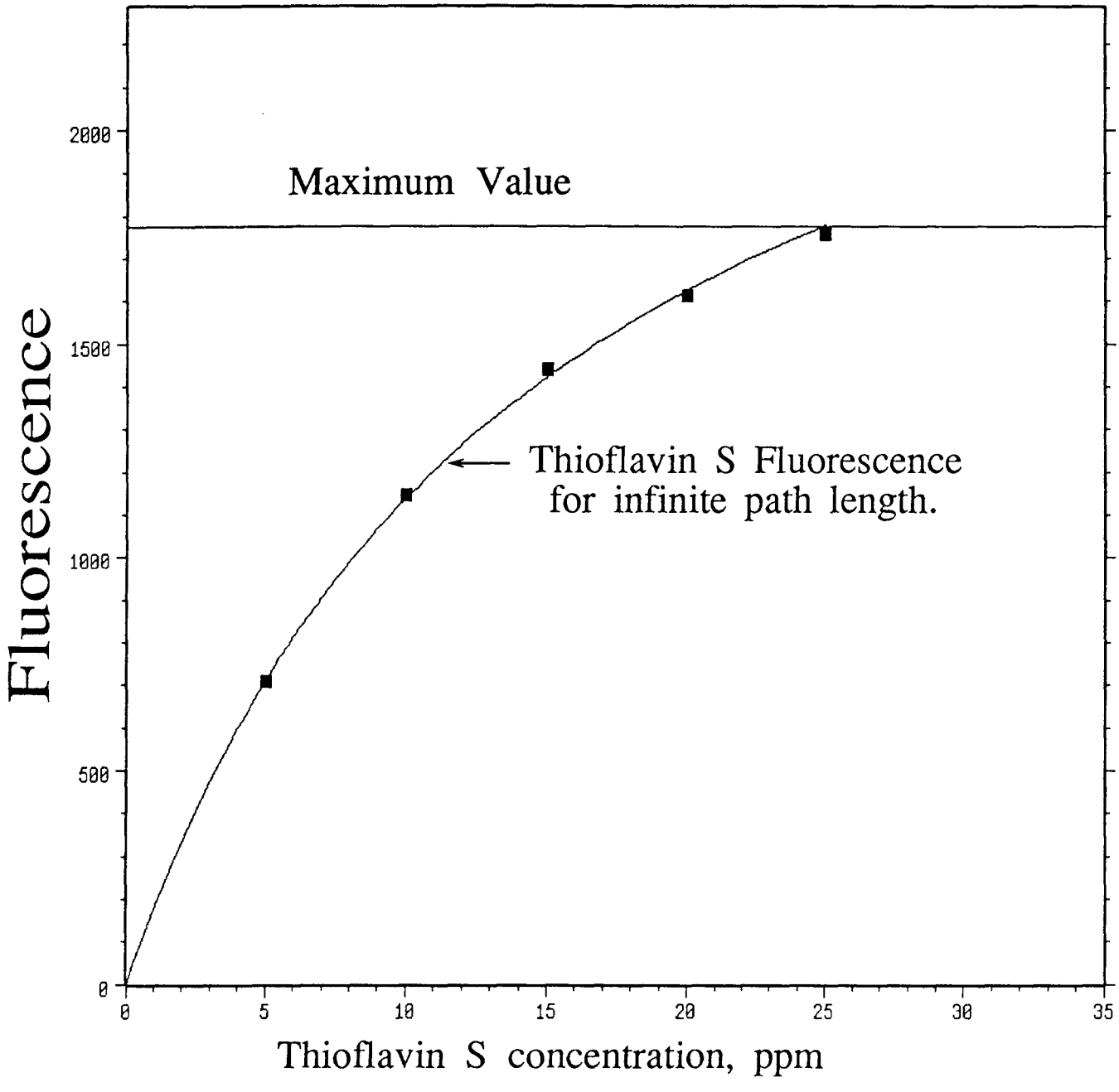

Figure 24: Variation of fluorescence signal with temperature for several fluorophores. Reproduced from [Udenfriend 1962]. In this case, probably all emission light was detected, instead of limiting the detection to a narrow band, as is the case with the FluroMeasure^{TM} probe. The expected result for the detection of a narrow band is shown in Figure 25.

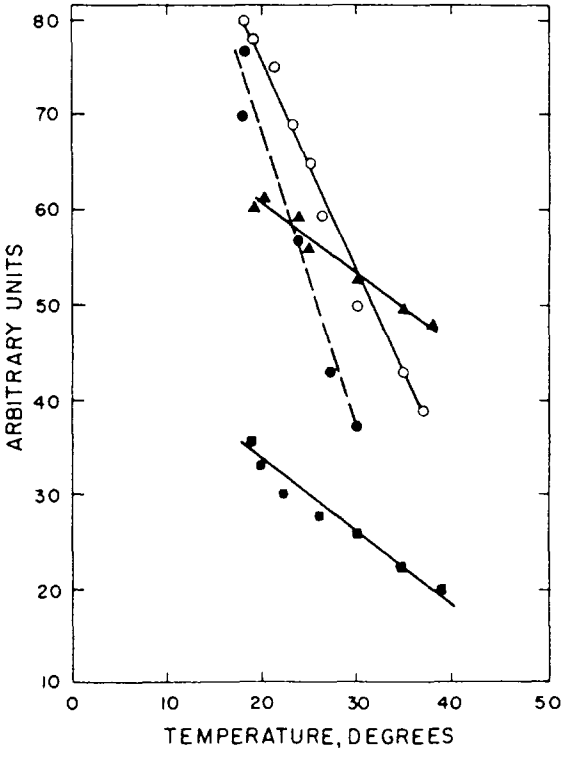

Variations in fluorescence intensity of several compounds as a function of temperature. All compounds were dissolved in 0.1 *M* phosphate buffer, pH 7.0, except quinine (J. Green, unpublished observations). ○ — ○, tryptophan or indoleacetic acid; ● — ●, indoleacetic acid in buffer saturated with benzene; ▲ — ▲, tyrosine; ■ — ■, quinine in 0.1 *N* sulfuric acid.

Figure 25: Possible effects of temperature on the fluorescence signal. At λ_1, the fluorescence decreases, while at λ_2, the fluorescence increases.

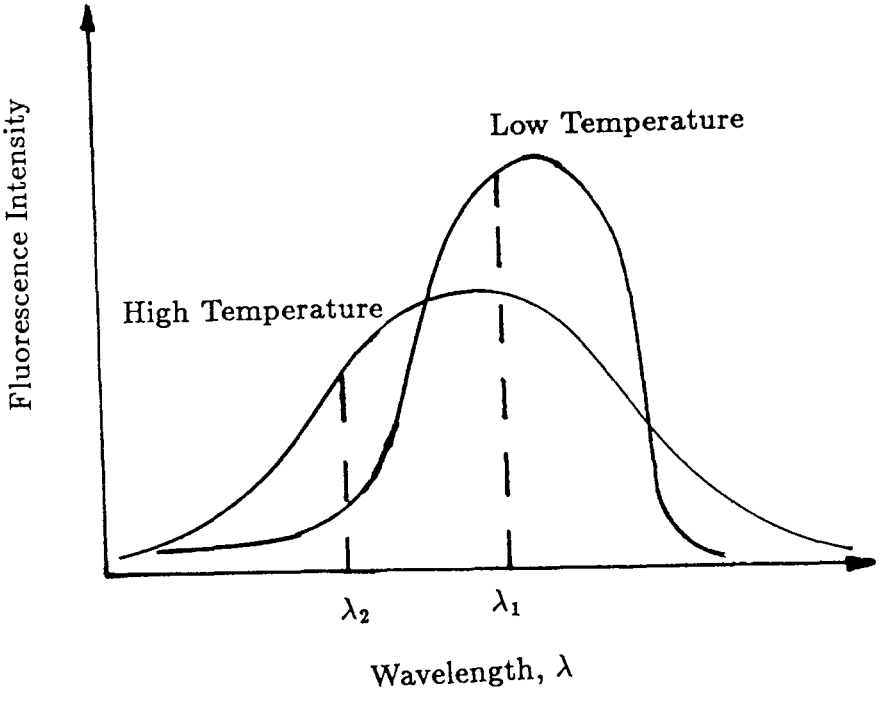

Figure 26: Oscillations of the culture fluorescence signal due to oscillations in temperature in a batch culture of *Bacillus amyloliquefaciens* during sporulation. The sensitivity to temperature was found to be $2.6\frac{\text{NFU}}{^\circ\text{C}}$ in this case.

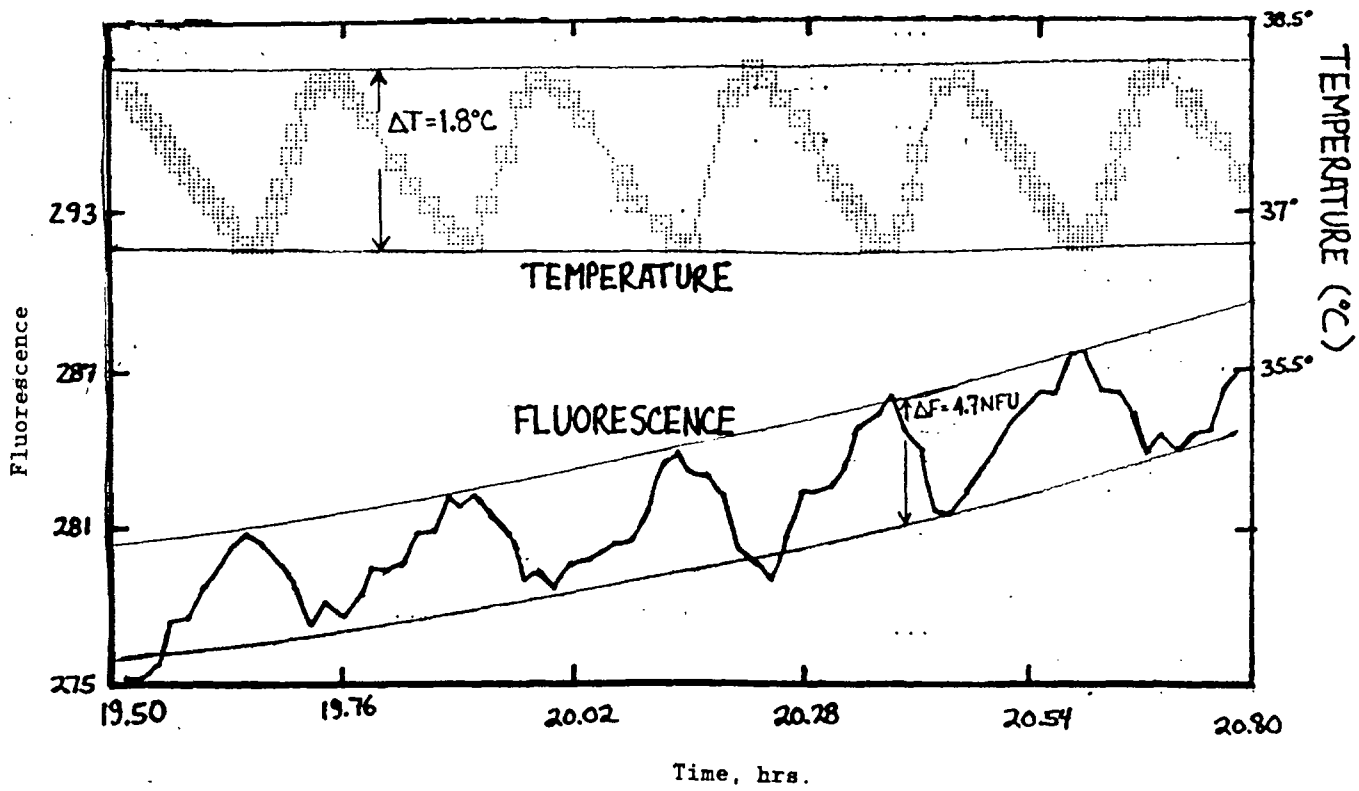

Figure 27: Typical dependence of fluorescence on pH. Reproduced from [Udenfriend 1962].

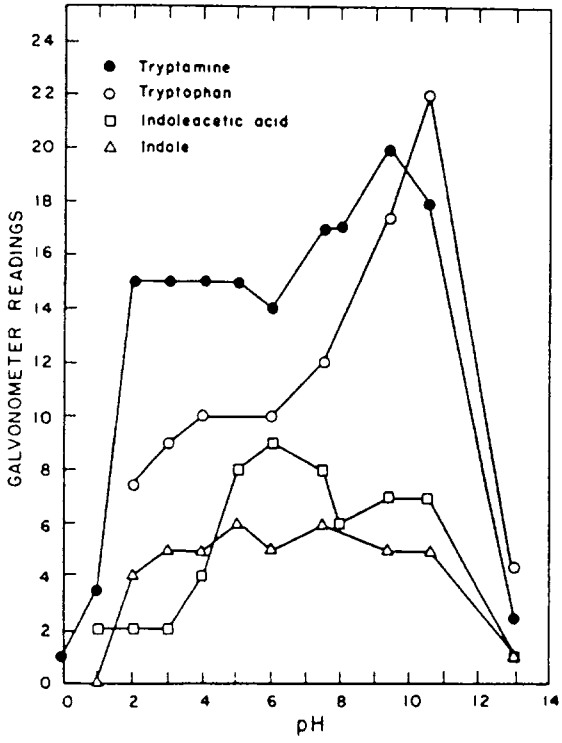

Effect of pH on the fluorescence of tryptophan and related compounds.

Figure 28: Some compounds that are fluorescent in only a particular form. Reproduced from [Udenfriend 1962].